Textures and Microstructures, 1996, Vol. 25, pp. 71–108
Reprints available directly from the publisher.
Photocopying permitted by license only

PHYSICAL VERSUS MATHEMATICAL ASPECTS IN TEXTURE ANALYSIS

H. J. BUNGE

Department of Physical Metallurgy, Technical University of Clausthal, Germany

(Received 4 December 1995)

Texture deals with the orientational aspects of the crystal lattice in polycrystalline aggregates. This comprises the classical orientation distribution function ODF as well as higher-order textural quantities. The quantitative treatment of these quantities requires a good deal of mathematical methods. This concerns particularly the representation of orientation data including all kinds of symmetries, the transformation of experimentally measured raw data into the required distribution functions, as well as mathematical models of texture formation by physical processes and of the texture-property relationship.

When physical facts are idealized in terms of a mathematical description or by mathematical models then the physical limits, within which these are valid, must be known. Such physical limits are, for instance, definition of crystal orientation by the crystal lattice which leads to an unsharpness relationship between location and orientation resolution as well as a relationship between statistical relevance and angular resolving power. Other physical limits are given by the "fuzzyness" of sample symmetry. A central problem is pole figure inversion i.e. the inversion of the projection equation. This problem may have a "physical" solution even if it does not have a mathematical one. Finally, in the problem of rationalizing orientation distribution functions in terms of a low number of "components", mathematical aspects may be quite different from physical ones.

In all these problems it is thus necessary to keep the mathematical aspects apart from physical aspects.

KEY WORDS: Polycrystalline aggregates, Orientation size, Location and angular resolution, Statistical relevance, Higher-order textural quantities, Symmetries, Fuzziness, Pole figure inversion, Discrete textures, Texture components.

INTRODUCTION

Texture as a distinct field of research may be dated back to the first monograph "Texturen metallischer Werkstoffe" by G. Wassermann (1939). At that time the experimental technique of texture measurement was based on photographic films which were evaluated qualitatively into pole "figures". Later on the film was replaced by a Geiger-Müller counter. This made the quantitative determination of *pole density distribution functions* possible which allowed and required mathematical treatment.

Pole density distributions are supperpositions of pole densities from crystals with different orientations which are not distinguished by the diffraction process in a polycrystal. In order to resolve this ambiguity the procedure of "pole figure interpretation" was used. This means, it was tried to find "ideal orientations" with some spread about them, the superposition of which lead to the experimentally obtained "quantitative pole figures". This procedure worked quite well as long as the orientation distribution consisted of not too many ideal orientations with not too broad spread about them. Nevertheless, it was, at the best, semiquantitative.

The availability of quantitative pole density distributions asked for a mathematical solution of the projection problem. This was done about (1965) by several authors using different mathematical approaches (Bunge 1965, Roe 1965, Williams 1968). This way, the orientation distribution function (ODF) became available as a quantitative distribution function which could then be further used in quantitative mathematical treatments of texture-related problems. These were mainly mathematical models of physical processes by which textures are being formed as well as models of physical properties of polycrystalline aggregates.

Since crystal orientation requires three parameters for its complete description the orientation distribution function is a function in a three-dimensional space which has a non-Euclidian metric. Also symmetries must be taken into consideration. Hence, the mathematical foundation of many texture-related problems became necessary. Furthermore, the angular resolving power of the ODF and hence of the measured pole figures had to be increased. This makes the measurement and further "handling" of an increasing amount of data necessary. These data were made available by automatisation of texture goniometers and, most recently, by the use of "parellel detectors" e.g. Position Sensitive Detectors, Area Detectors, Energy Dispersive Detectors, and even the combination of these detection principles. Hence, mathematical methods of handling, "condensation", and evaluation of large data sets became necessary. Modern texture analysis is thus unthinkable without more and more sophisticated mathematical methods.

The early developments of "Texture Mathematics" were - so to speak - "home-made" by experimental physicists. In an advanced state this is no more sufficient so that increasingly theoretical physicists and mathematicians become involved in this field.

The classical term "Texture" as defined by the orientation distribution function (ODF) does not contain any information about size, shape, and mutual arrangement of the crystallites of the considered polycrystalline aggregate. Mathematically speaking, it is a "projection" of a six-dimensional "orientation-location" space into the three-dimensional orientation space. Another projection is the three-dimensional "location-space" i.e. the "natural space" considered in the different branches of stereology (e.g. quantitative metallography). The availability of new experimental techniques with extremely increased location as well as angular resolution (e.g. electron diffraction and synchrotron radiation) makes it necessary to go into the six-dimensional "orientation-location" space and to develop appropriate new mathematical methods for that. This characterizes the present situation in the field of textures. It is selfsaying that this increases the amount of data to be handled by many orders of magnitude.

From the very beginning of "Texture Mathematics" i.e. the interpretation of pole density distribution functions by "ideal orientations" up to the most advanced mathematical methods of "pole figure inversion" always idealized mathematical models had to be used which are then confronted with systematic and statistical errors. This applies, on the one hand, to *experimental errors*. On the other hand, however, it applies also to the very *definition* of the considered quantities. Polycrystalline aggregates have a stochastic nature which becomes more and more evident, the more we are able to increase angular and location resolution. In the ultimate limit each sample has its own "personal" aggregate structure and is representative only for itself. In some cases we may be interested in that. In some other cases, however, we are looking for "statistically relevant" parameters characterizing the whole charge of material. From the technological aspect most often such parameters are required. It is clear that this latter aspect requires to neglect some individual aspects. This may seem to be incorrect. But also the opposite situation may be encountered. From a mathematical aspect it may seem meaningful

to consider, for instance, certain prominent classes of distribution functions as being representative for texture functions. From the physical aspect this may be incorrect if also other classes of functions are experimentally observed.

Hence, it is always necessary to take both aspects - mathematical and physical ones into account.

It is the purpose of the present paper to compare mathematical versus physical aspects in texture analysis in some illustrative examples.

MATHEMATICAL ASPECTS IN TEXTURE ANALYSIS

Texture analysis deals with polycrystalline aggregates of which it considers particularly the orientational aspect. The aggregate structure influences the macroscopic *properties* of the materials. On the other hand, the aggregate structure is formed by anisotropic solid state *processes*. Both these relationships: "Processes ⟶ Texture" and "Texture ⟶ Properties" must be understood in terms of mathematical models including texture, respectively the whole aggregate structure. In technological applications both aspects must be considered. In many cases both aspects are mutually interrelated as for instance in metal forming processes, e.g. deep drawing. Hence, mathematical models taking both into account (i.e. feed-back models) are needed.

Textures and other aggregate parameters must be measured. Thereby more and more advanced techniques are used. Hence, data evaluation by mathematical methods is necessary.

Finally, as was already mentioned, the mathematical representation of texture and other aggregate parameters requires mathematical methods. Hence, the implications of mathematics in texture analysis may be summarized in the scheme given in Figure 1.

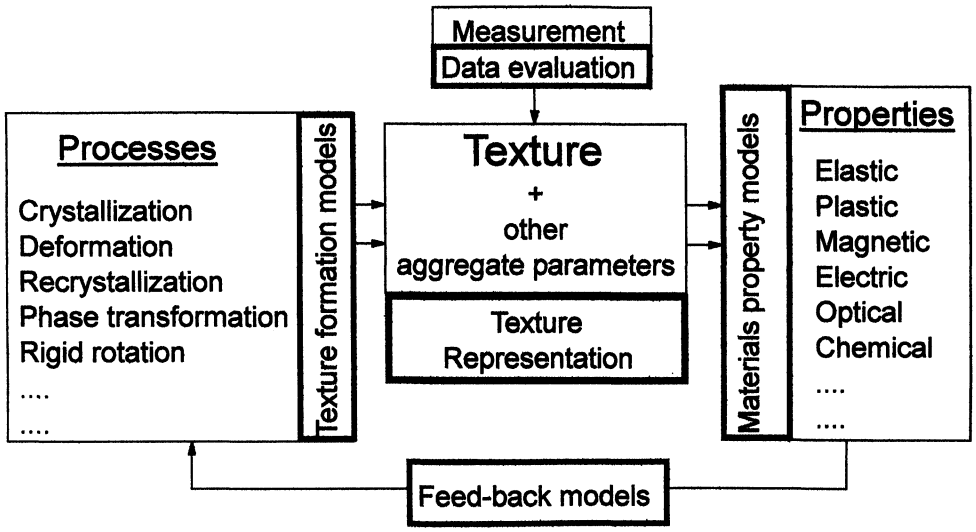

Figure 1 Fife main areas of mathematical methods used in the field of texture. Data evaluation. Texture representation. Texture-formation models. Texture-property models. Feed-back models.

CRYSTAL ORIENTATION

The central quantity in texture analysis is crystal orientation. In order to define it, a crystal-fixed coordinate system K_B must be related to a sample-fixed one K_A. If we assume at first that both coordinate systems are chosen right-handed then this relationship is a rotation g, Figure 2.

$$K_B = g \cdot K_A \tag{1}$$

The rotation g can be specified in many different ways e.g. by a transformation matrix, by Miller indices, by rotation axis and angle, or by Euler angles

$$g = [g_{ik}] = (hkl)[uvw] = \{\vec{r}, \omega\} = \{\varphi_1 \phi \varphi_2\} \tag{2}$$

The transformations between these coordinates can easily be given (Bunge, 1969, 1982, Hansen, Pospiech, Lücke 1978). Particularly we consider here the representation by Euler angles. They can vary in the range

$$0 \leq \varphi_1, \varphi_2 \leq 2\pi, \quad 0 \leq \phi \leq \pi \tag{3}$$

and are repeated periodically outside this range. An orientation is thus represented by a point in this space, i.e. the Euler space. According to the metric of the Euler space, equivalent volume elements are defined by

$$dg = \frac{1}{8\pi^2} \cdot \sin \phi \, d\phi \, d\varphi_1 \, d\varphi_2 \tag{4}$$

The so defined Euler space has the finite volume

$$G = \oint dg = 1 \tag{5}$$

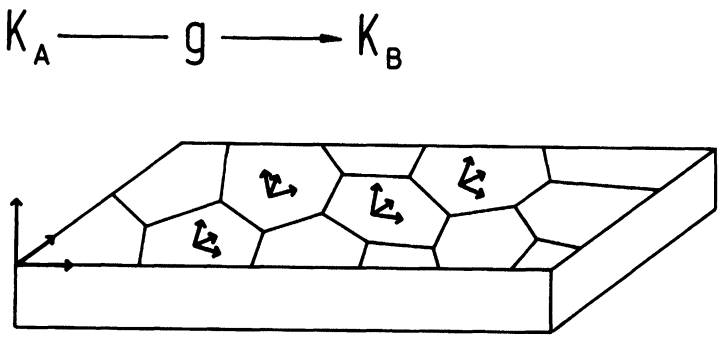

Figure 2 Crystal orientation defined by the rotation g which brings the sample coordinate system K_A into coincidence with the crystal coordinate system K_B.

Orientation size

In order to define the crystal coordinate system K_B, a crystal lattice must exist. In the mathematically strict sense the ideal crystal lattice extends to infinity. In physical reality, however, it is finite, the absolute lower limit being just one unit cell. The coordinate axes are then fixed by rows of atoms, the positions of which are not fixed points in the mathematical sense. We may assume that they are defined only within a certain fraction ϵ of the lattice parameter a Figure 3. If the dimension of the crystal (in the direction of a) is n unit cells then this direction can only be defined with the uncertainty

$$\Delta\alpha = \frac{\epsilon \cdot a}{n \cdot a} = \frac{\epsilon}{n} \tag{6}$$

The diameter of this crystal in the direction of a is

$$d = n \cdot a \tag{7}$$

Hence, the orientation of a crystal of size d can only be specified with the uncertainty

$$\Delta\alpha = \frac{\epsilon \cdot a}{d} \qquad (\epsilon \cdot a \sim 1\text{Å}) \tag{8}$$

The orientation of a finite crystal must thus be represented by a *volume* in the orientation space with the diameter $\Delta\alpha$ rather than by a *point*. Hence, crystal size d defines an "orientation size" $\Delta\alpha$ according to eq(8) as is illustrated in Figure 4.

If the crystal has anisotropic shape, e.g. it is a needle, then one of two Euler angles is more "diffuse" than the other two. If we assume that the needle axis is the x_3 axis of the crystal coordinate system K_B then this is the Euler angle φ_2, as is illustrated in Figure 5. The orientation "point" of this crystal is then elongated in the φ_2-direction. Crystals which are small only in one direction i.e. plates do not show this effect. The two directions in the plate already fix the orientation with an accuracy corresponding to their size in these directions. Hence, the orientation "point" of a plate is spherical as is also shown in Figure 5. Finally this figure shows orientation "points" of big and small crystals.

We consider crystal size d in three mutually perpendicular crystal directions then the crystal volume is given by

$$v = d^3 \tag{9}$$

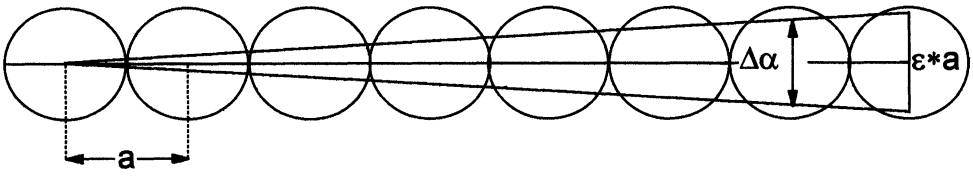

Figure 3 Illustration of the uncertainty $\Delta\alpha$ of crystal orientation.

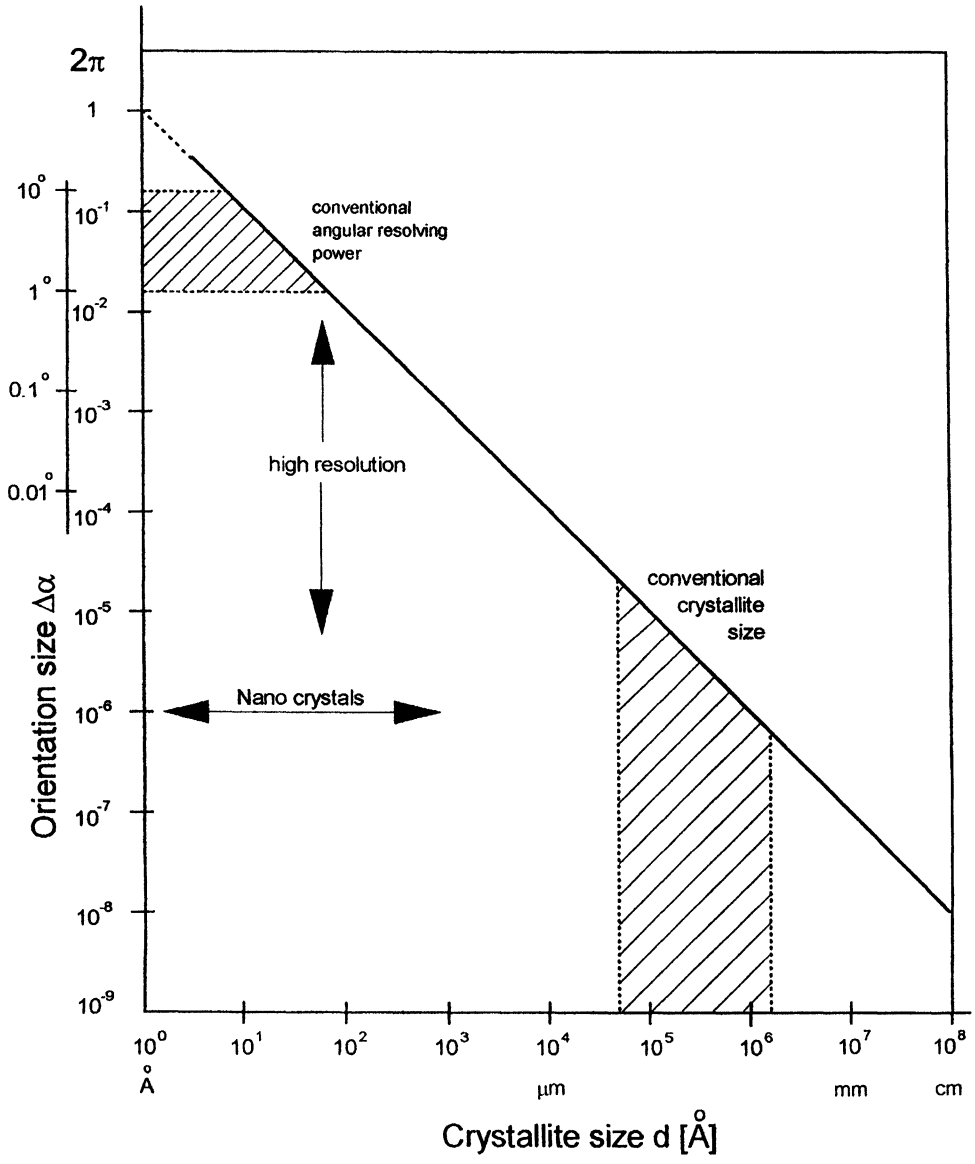

Figure 4 Relationship between crystallite size d and orientation size $\Delta\alpha$ (eq(8)).

Analogously we define orientation size $\Delta\alpha$ in three mutually perpendicular directions in the orientation space. Taking the normalization of this space, according to eq(4) and eq(5), into account we obtain the "orientation volume" Δg for that crystal

$$\Delta g = \frac{1}{8\pi^2}\Delta\alpha^3 = \frac{1}{8\pi^2}\sin\phi\Delta\phi\Delta\varphi_1\Delta\varphi_2 \tag{10}$$

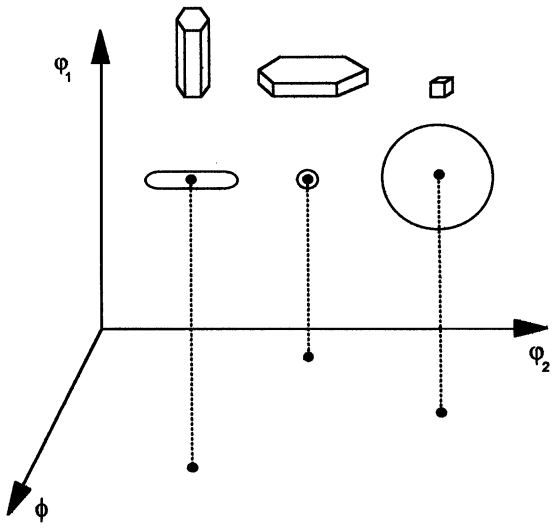

Figure 5 Anisotropic sizes of crystals and their representative volume elements in the orientation space.

We thus obtain from eq(8)

$$\Delta g \cdot v = \frac{\epsilon^3 \cdot a^3}{8\pi^2} \qquad (\epsilon \cdot a \sim 1\mathring{A}) \tag{11}$$

where v is the volume of a crystal in real space and Δg is the volume occupied by its orientation g in the orientation space.

STRUCTURE OF POLYCRYSTALLINE AGGREGATES

The structure of a polycrystalline aggregate can be completely described by specifying crystal orientation $g = \{\varphi_1 \phi \varphi_2\}$ in each location $\vec{x} = \{x_1 x_2 x_3\}$ of the sample as is illustrated in Figure 6. Then the aggregate function

$$g = g(\vec{x}) \begin{cases} \varphi_1 = \varphi_1(x_1 x_2 x_3) \\ \phi = \phi(x_1 x_2 x_3) \\ \varphi_2 = \varphi_3(x_1 x_2 x_3) \end{cases} \tag{12}$$

describes the aggregate completely.

The unsharpness relationship between location and orientation

In order to specify the orientation of a crystal in the location $\vec{x}$, a crystal lattice must be specified in this location. Hence, the lower limit for the uncertainty Δx of a location point $\vec{x}$ of a crystal is one unit cell. If, however, orientation is to be specified with higher accuracy then the crystal lattice must extend over a longer distance. The "location" of this lattice is then defined with an uncertainty Δx in the order of the size d of the corresponding crystallite. Hence, the uncertainties Δx of location and $\Delta\alpha$ of orientation are related to each other by an "uncertainty relation" according to eq(8)

$$\Delta\alpha \cdot \Delta x = \epsilon \cdot a \sim 1\mathring{A} \tag{13}$$

With eq(10) this can also be expressed in terms of a volume element ΔV in the location space and a volume element Δg in the orientation space

$$\Delta g \cdot \Delta V = \frac{\epsilon^3 \cdot a^3}{8\pi^2} \qquad (\epsilon \cdot a \sim 1\mathring{A}) \tag{14}$$

If the sample has the total volume V then it contains

$$N_v = \frac{V}{\Delta V} \tag{15}$$

such volume elements, in each of which

$$N_g = \frac{G}{\Delta g} = \frac{1}{\Delta g} \tag{16}$$

different orientations can be distinguished. Hence, the total number of distinguishable aggregates in a sample with the volume V is

$$N_{aggr.} = N_v \cdot N_g = \frac{8\pi^2}{\epsilon^3 \cdot a^3} \cdot V \qquad (\epsilon \cdot \mathrm{a} \sim 1\mathring{A}) \tag{17}$$

Different types of aggregate functions

The aggregate function may have different forms depending on the type of microstructure considered. This is shown schematically in Figure 7. Recrystallized materials may consist

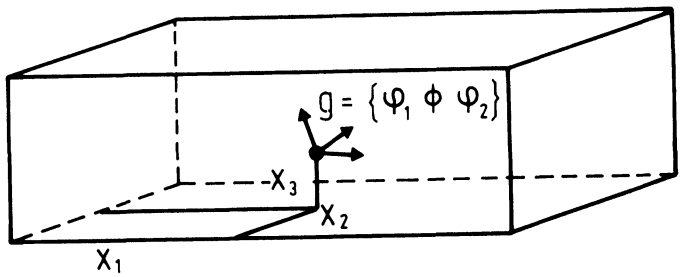

Figure 6 Illustrating the definition of the aggregate function $g(\vec{x})$.

of well developed grains with constant orientation inside and with high-angle grain boundaries between them. In other cases there may also be low-angle boundaries inside the crystallites. Finally, there may be a complicated dislocation microstructure in the crystals. This may lead to lattice distortions and hence to continuous orientation changes.

Grain boundary networks

In the case illustrated in Figure 7a i.e. big, well developed grains, an alternative description to that of eq(12) by the aggregate function is possible. It is then sufficient to specify the orientations g_i of grains and the positions of all grain boundaries between them by the total grain boundary function

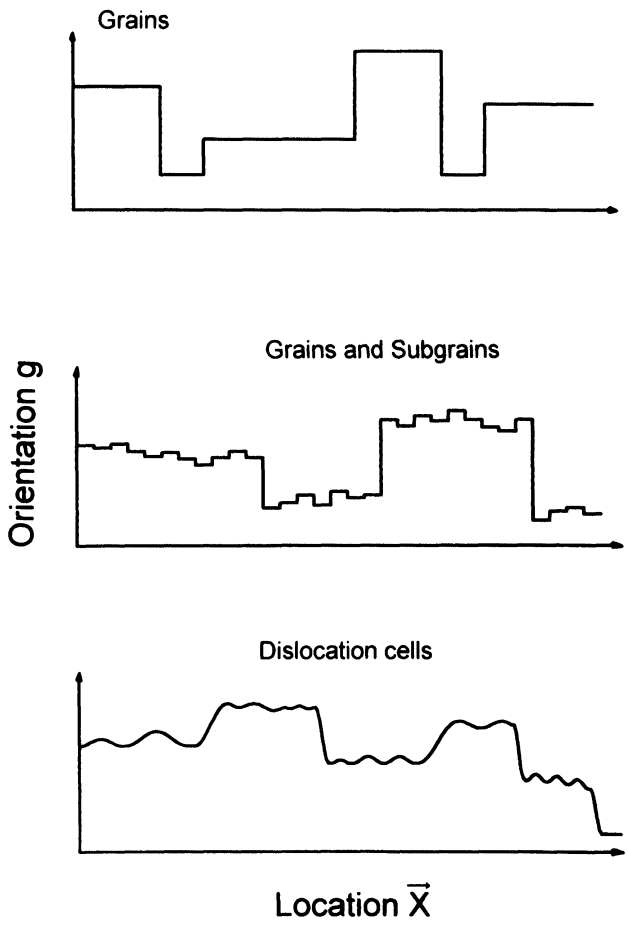

Figure 7 Three types of aggregate functions
a) big, well-developed grains
b) big grains with low-angle boundaries inside
c) curved crystal lattice due to dislocation substructure.

$$F(x_1 x_2 x_3) = 0 \tag{18}$$

Each pair of adjacent grains defines a grain boundary (which is part of the function F). Each triple of adjacent grain boundaries defines a grain edge. Each quatruple of adjacent edges defines a grain corner. If, in a further specification, all grain boundaries are plane then the total grain boundary network is completely fixed by the corner points

$$\vec{x}_{corn.} = \{x_1 x_2 x_3\}_i \tag{19}$$

and the specification which ones are connected. Also this alternative description of an aggregate is a complete one which is representative only for one particular sample.

STATISTICAL DESCRIPTION OF THE AGGREGATE STRUCTURE

The complete description of the aggregate function, on the one hand, requires very many data, on the other hand it is representative only for one specific sample. This is often not desirable. Hence, statistical descriptions of the aggregate structure are being looked for.

The classical texture - ODF

The "first-order" statistical quantity that can be defined in all three types of microstructures shown in Figure 7 is the orientation distribution function ODF. It considers only the orientations of crystals or crystalline volume elements and neglects completely any location coordinates. It is

$$\frac{dV/V}{dg} = f(g); \qquad \begin{matrix} g = \{\varphi_1 \phi \varphi_2\} \\ dg = \frac{1}{8\pi^2} \sin\phi \, d\phi \, d\varphi_1 \, d\varphi_2 \end{matrix} \tag{20}$$

It is a statistical distribution function of crystallites or volume elements which is characterized by an angular resolution and a statistical relevance, shown schematically in Figure 8.

Statistical relevance and angular resolving power

The statistical relevance is limited by the total number N of crystallites which contribute to the value $f(g)$ within the (finite) orientation element Δg. Hence, relevance and resolving power are closely related. The relevance may be defined by

$$\frac{\Delta f}{f} = \frac{\sqrt{N}}{N} = \frac{1}{\sqrt{N}} \tag{21}$$

With a crystal diameter d and a sample diameter D it is

$$N = \left[\frac{D}{d}\right]^3 \cdot f(g) \cdot \Delta g \tag{22}$$

and hence

$$\frac{\Delta f}{f} = \sqrt{\frac{d^3/D^3}{f(g) \cdot \Delta g}} = \sqrt{\frac{8\pi^2 d^3/D^3}{f(g) \cdot \Delta \alpha^3}} \tag{23}$$

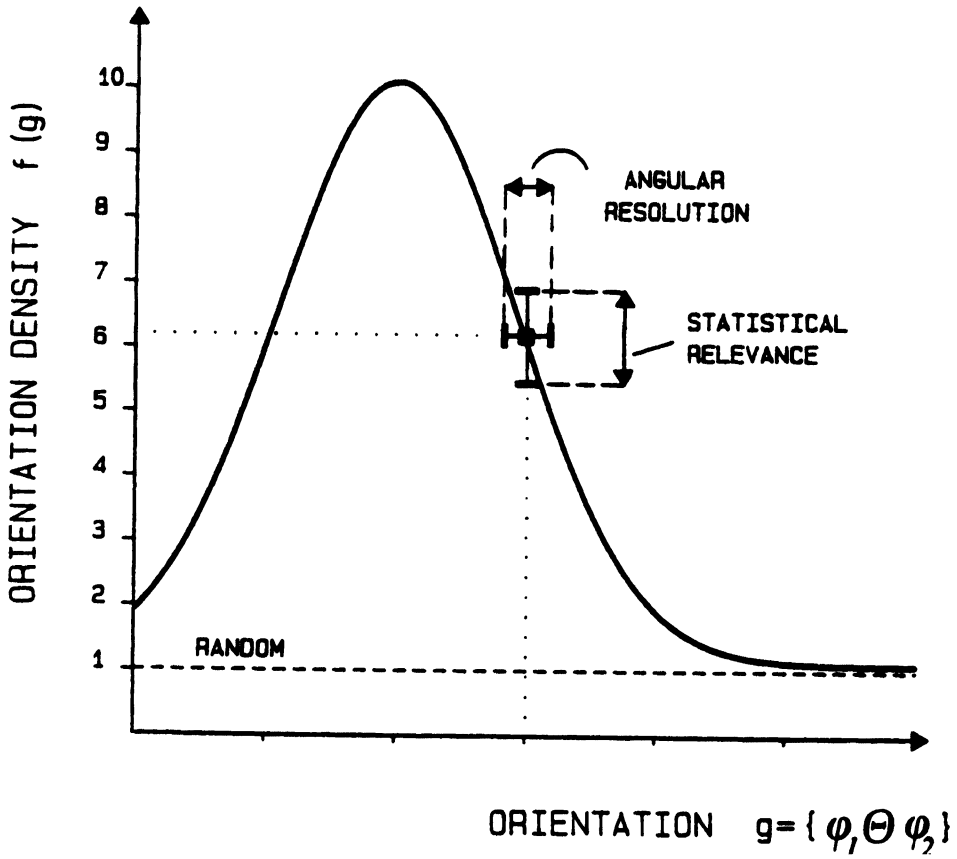

Figure 8 Angular resolving power and statistical relevance of the orientation distribution function f(g) (one-dimensional).

This is illustrated in Figure 9 as a function of the angular resolving power $\Delta\alpha$ and for various ratios d / D, assuming $f(g) = 1$.

The highest possible relevance is obtained when the crystal diameter is taken as the smallest possible one for an assumed angular resolution $\Delta\alpha$ according to eq(8). We then obtain

$$\frac{\Delta f}{f} = \frac{1}{\Delta\alpha^3}\sqrt{\frac{8\pi^2 \cdot \epsilon^3 \cdot a^3}{f(g) \cdot D^3}} \tag{24}$$

This is illustrated in Figure 10 as a function of the angular resolving power $\Delta\alpha$ and for various sample diameters D, assuming random texture $f(g) = 1$. Comparing Figure 9 and Figure 10 it is seen that the statistical relevance can either be limited by grain size d or by orientation size, i.e. the maximum resolving power can be reached according to the given orientation size. In fact, only the lowest one of these two statistical relevances can be reached as is illustrated in Figure 11 for a particular sample size, i.e. 1 mm and a particular grain size, i.e. 10 nm. If, on the left-hand side of this figure, we would assume a situation on the dashed line, the relevance would be reduced by

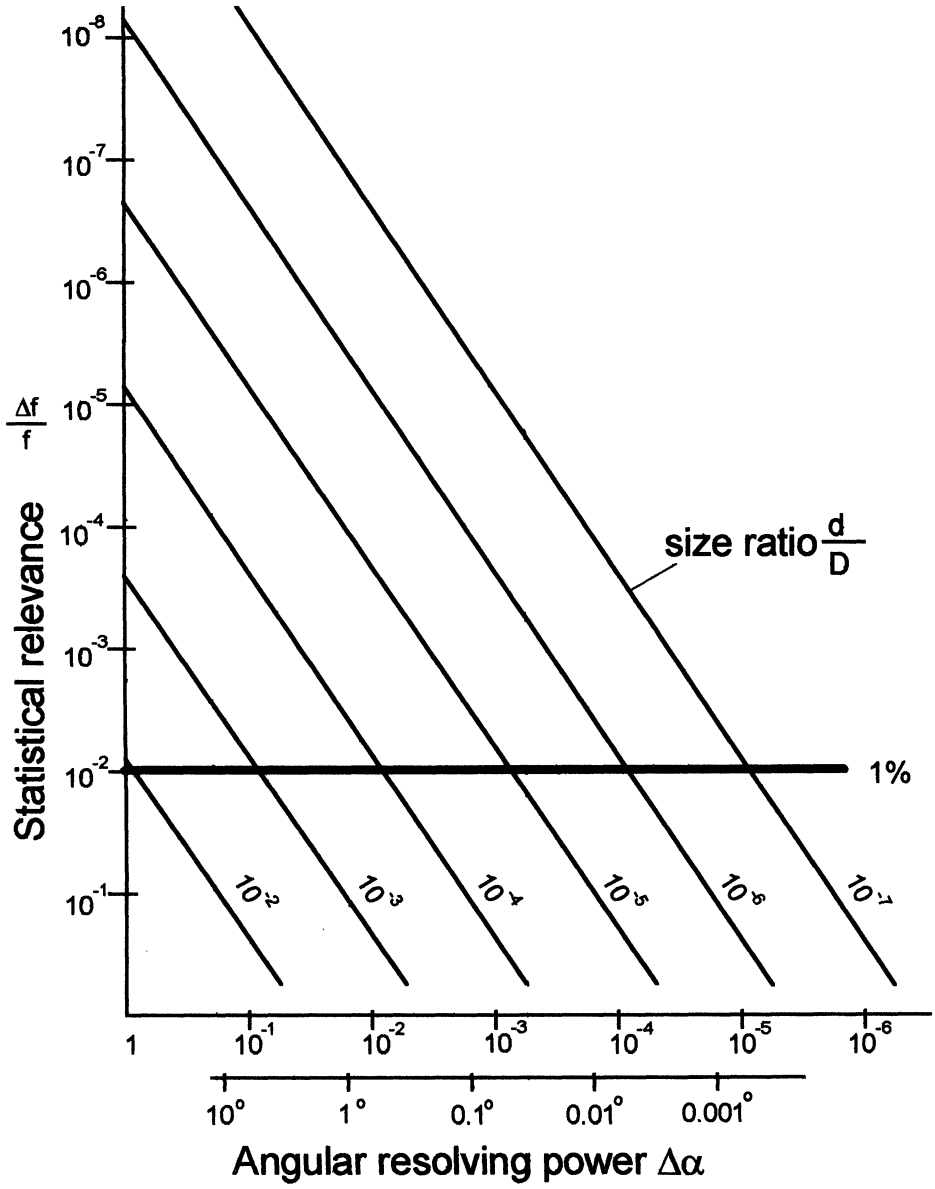

Figure 9 Relationship between statistical relevance and angular resolving power for the case of grain-size limited relevance (eq(23)). Parameter is the ratio d/D of grain to sample size.

grain statistics back to the full line. If, on the other hand, we would assume a situation on the dashed line on the right-hand side, then the actually reached resolving power would be that on the full line as indicated. The boundary point between the two lines is defined by eq(8) and by the line of Figure 4.

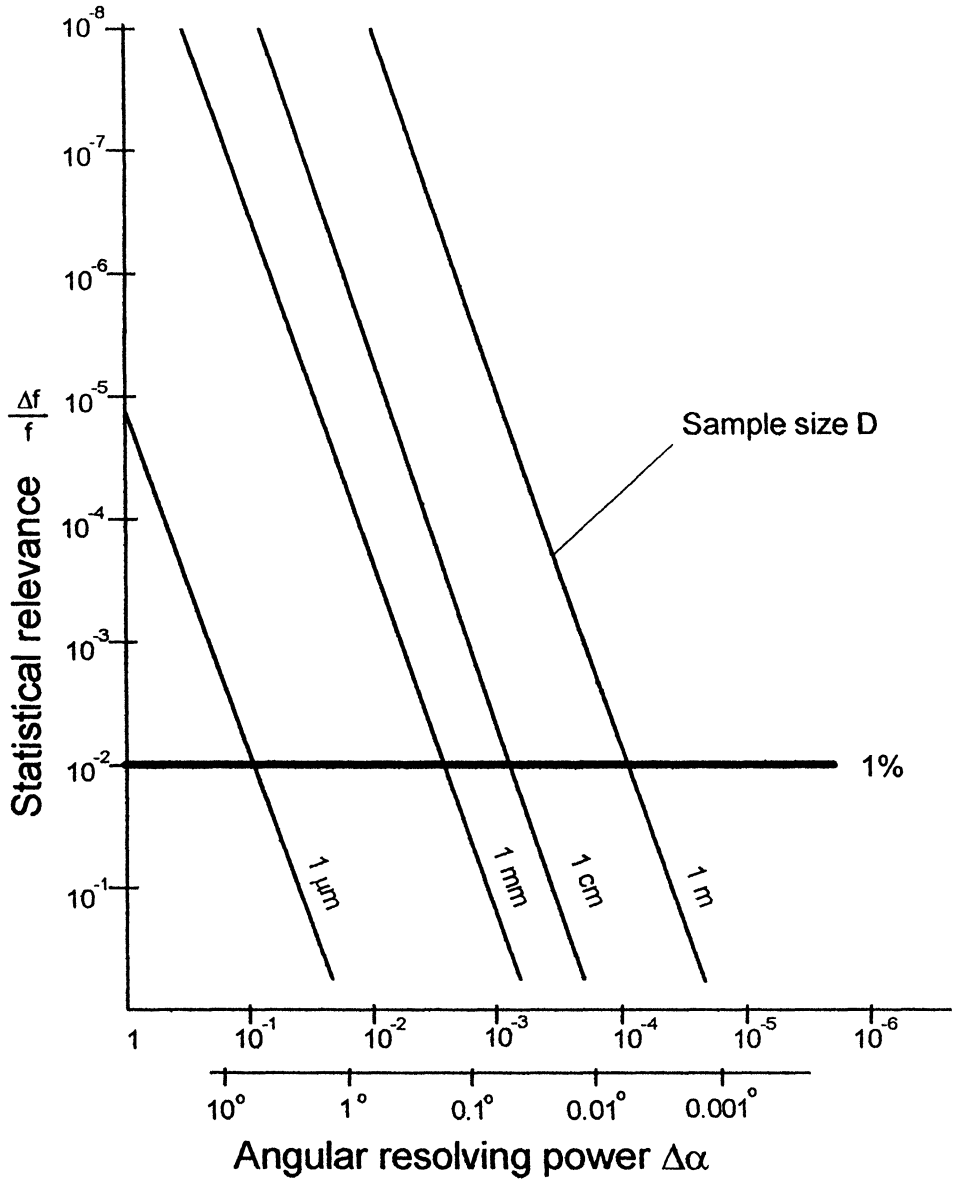

Figure 10 Relationship between statistical relevance and angular resolving power for the case of orientation-size-limited relevance (eq(24)). Parameter is the sample size.

Discrete versus continuous textures

Since the orientation space is finite, only a finite number of crystal orientations with a given orientation size can be resolved in it. If this is the case, we may call that a *discrete texture* (Each individual crystal orientation can be distinguished. This has

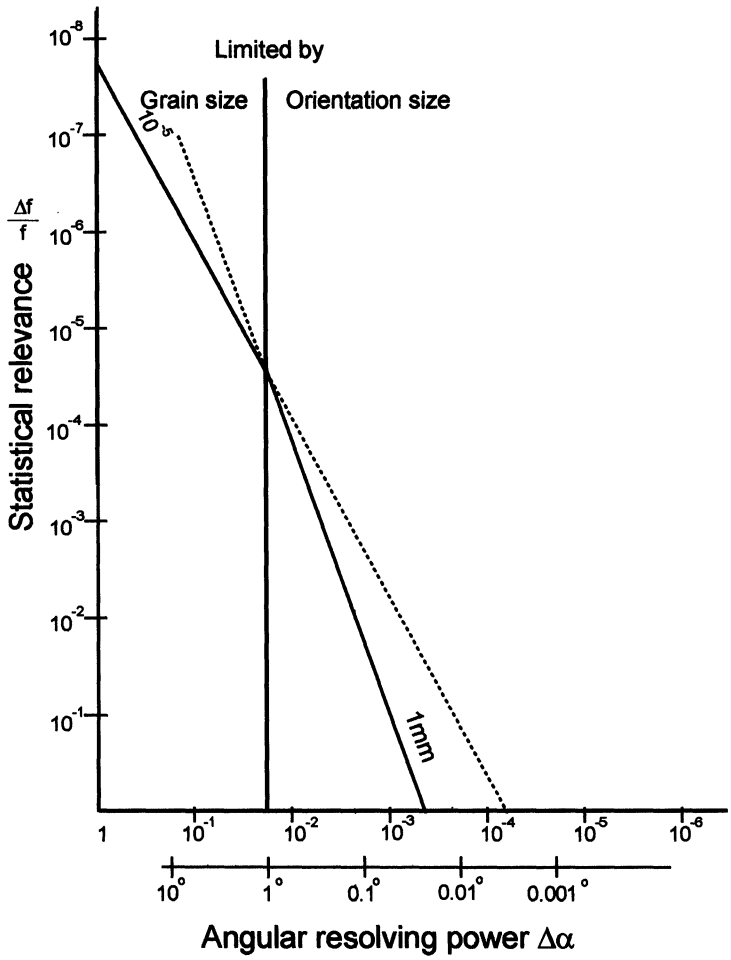

Figure 11 Relationship between statistical relevance and angular resolving power showing the ranges of grain-size limitation and orientation-size limitation (D = 1 mm, d = 10 nm).

also been called a "Multi-peak-texture" (Bunge, Morris, Nauer-Gerhardt (1989)). If the orientations (according to their orientation sizes) cannot be resolved the texture may be called *continuous*.

The maximum number of resolved orientation points with the orientation size Δg is given by

$$N_{max} = \frac{G}{\Delta g} = \frac{1}{\Delta g} \tag{25}$$

and expressing Δg by the crystal volume according to eq(11) it is

$$N_{max} = \frac{8\pi^2}{\epsilon^3 \cdot a^3} \cdot v \qquad (\epsilon \cdot a \sim 1\text{Å}) \tag{26}$$

This defines a critical sample size D_{crit} above which resolution is no more obtained. It is

$$D_{crit} = \sqrt[3]{N_{max}} \cdot d = \frac{\sqrt[3]{8\pi^2}}{\epsilon \cdot a} \cdot d^2 \tag{27}$$

Above this size the texture is "continuous" below it the texture is "discrete". Figure 12 gives the critical sample size as a function of crystallite size with the assumption $\epsilon \cdot a = 1\mathring{A}$. It is seen that for "conventional" crystallite sizes it is always possible to reach resolution of each individual crystallite i.e. the "multi-peak-texture" situation.

Higher-order textural quantities

Higher-order textural quantities can be defined by taking some information about location coordinates $\vec{x}$ into account additional to the orientation coordinates $g = \{\varphi_1 \phi \varphi_2\}$. This can be done in a great number of different ways depending on the type of microstructure illustrated for instance in Figure 7 (see e.g. Bunge 1994).

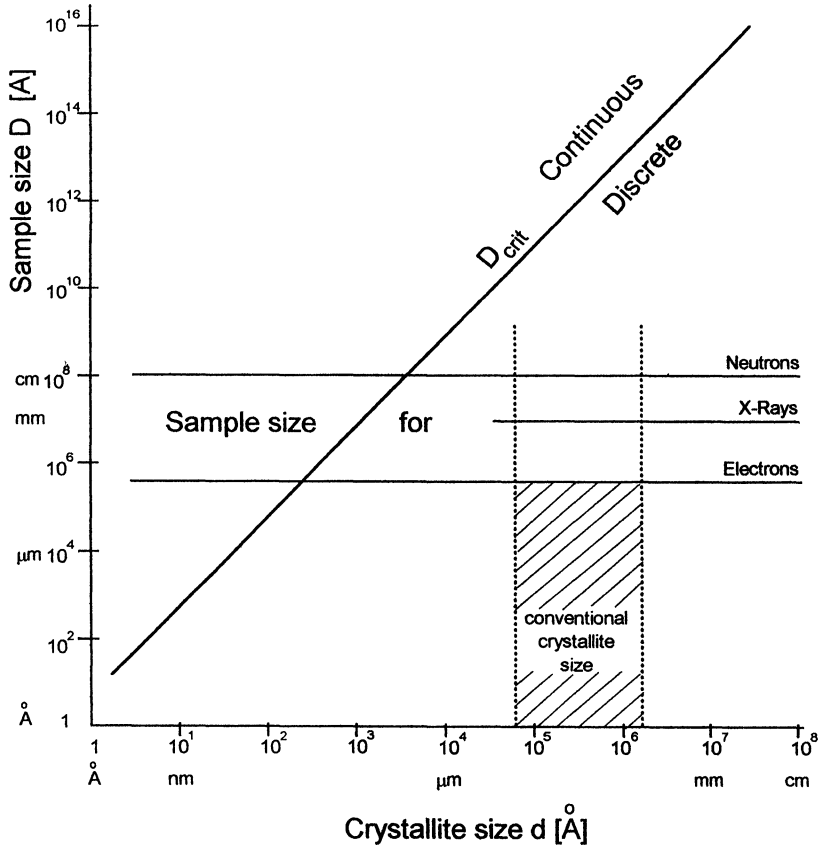

Figure 12 Discrete and continuous textures depending on crystallite size and sample size (eq(27)).

In the case of grain boundary network structures statistical distribution functions of the boundaries, edges, corners with respect to their characteristics parameters can be specified as is illustrated in Figure 13. These parameters are the orientations g_i of the crystals adjacent to each of these entities as well as the boundary normal directions and the edge directions. Hence, an increasing number of angular parameters is needed to describe these entities (ie. 8, 14, 20 respectively, compared with three for the ODF). Hence, the statistical distributions of grain boundaries, edges and corners are to be described in eight-, fourteen- or twenty-dimensional orientation spaces, respectively. The necessary number of data points in such spaces (assuming low-resolution i.e. 10 points for each coordinate or high-resolution i.e. 100 points) is shown in Figure 14. It is compared with the number of data points needed for the complete description of the aggregate function eq(12) in one, two or three dimensions. It is seen that there is always a "break-even point" where the statistical description requires more data points than the complete one. It must, however, be emphasized once more, that the number of data points is not the only argument in the decision whether complete or statistical description should be used. A very important argument is also that the complete description, strictly speaking, is valid only for one specific sample whereas the statistical description is valid for the whole material (in a statistical sense).

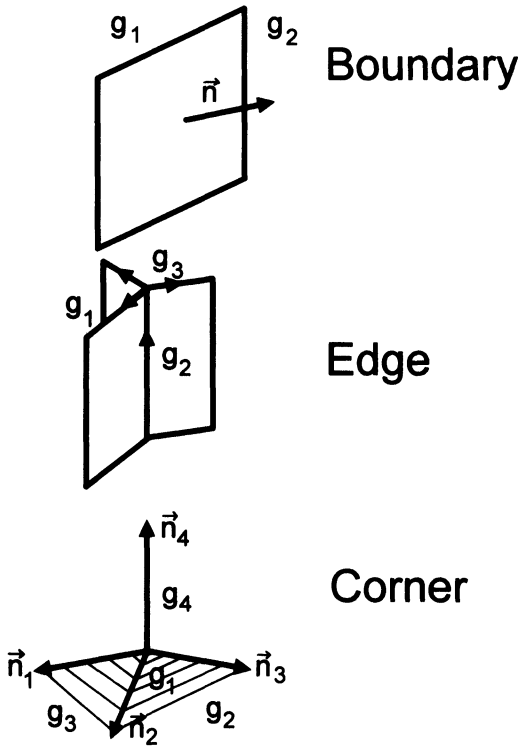

Figure 13 Entities of grains structures, i.e. grains, boundaries, edges, and corners and their respective orientation parameters.

The misorientation distribution function MODF

The lowest one among the higher-order textural quantities is the misorientation distribution function (MODF) of the grain boundaries (Bunge, Weiland 1988). It neglects the orientation of the normal direction of the boundary and considers only the misorientation between the two neighbouring grains, the orientations of which may be g_1 and g_2. The MODF is defined by

$$\frac{dA/A}{d\Delta g} = F(\Delta g) = F\{\varphi_1 \phi \varphi_2\} \qquad \begin{array}{l} \Delta g = g_2 \cdot g_1^{-1} \\ \Delta g = \{\varphi_1 \phi \varphi_2\} \end{array} \tag{28}$$

Thereby dA / A is the area fraction of boundaries having the misorientation Δg[††]. From the mathematical point of view, the MODF is very similar to the ODF. Particularly, angular resolving power and statistical relevance must be considered analogous to the case of ODF.

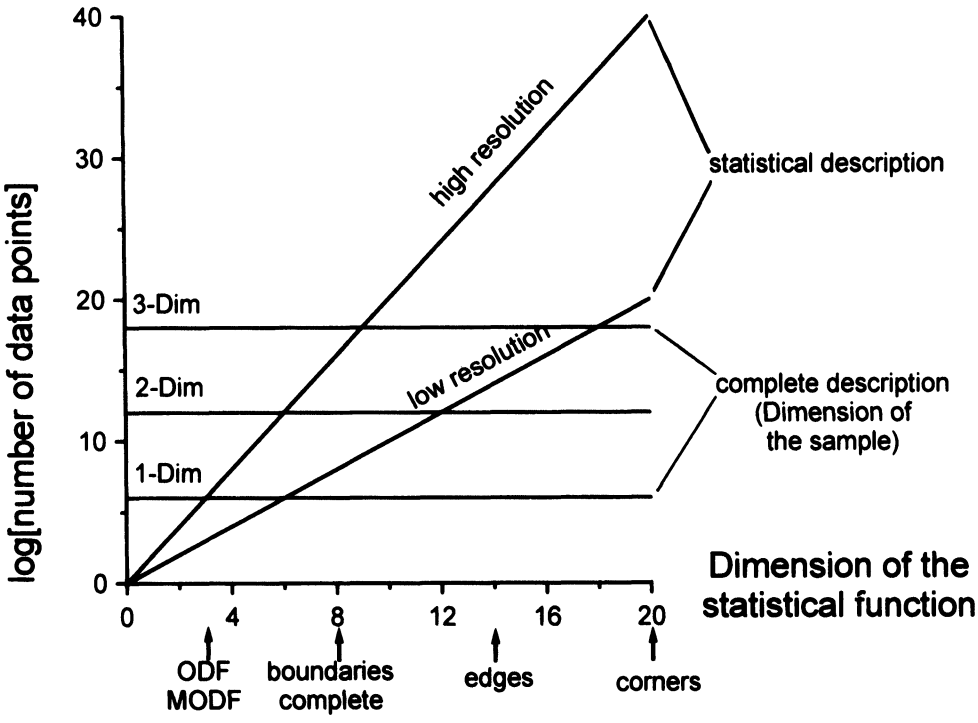

Figure 14 Number of data points needed for the complete and statistical description of a polycrystalline aggregate.

[††]Δg has another meaning than in eq(10)

SYMMETRIES IN TEXTURES

Texture deals with crystals which are highly symmetric objects by themselves, and also the arrangement of these objects in space may be highly symmetric. Hence, crystal and sample symmetry play a prominent role in texture analysis.

Crystal symmetry - orthogonal transformations

An ideal crystal can be brought into coincidence with itself by several kinds of symmetry operations. These are

- translations t^c
- rotations g^c
- inversional symmetries u^c

$\Big\}\, o^c$

as well as combinations of these. After carrying out any of these symmetry operations the resulting crystal is indistinguishable from the starting one. It must be considered as being the *same* crystal.

In the orientation distribution function (ODF) we do not consider the location of a crystallite. Hence, translational symmetries need not to be taken into account.

In the classical definition of the ODF, eq(20), crystal orientation is described by a rotation g. Hence, symmetry *rotations* g^c can easily be taken into account. Inversional symmetry elements u^c cannot be taken into account in this way. They transform a right-handed reference system into a left-handed one. This is not possible in the conventional definition of the ODF. It is, however, desirable to take all symmetries of the crystal class i.e. the point group symmetry into account. Hence, crystal orientation must be defined in a more general way by a general orthogonal transformation o (including inversional elements which lead from right-handed to left handed reference systems) (Esling, Bunge, Muller 1980). We define the ODF in the more general form

$$\frac{dV/V}{do} = f(o) = \{f^r(g),\, f^i(u)\} \qquad \begin{matrix} r = \text{rotational} \\ i = \text{inversional} \end{matrix} \tag{29}$$

In this function two ranges, the g-range and the u-range can be distinguished as is shown schematically in Figure 15. This function must be invariant with respect to all symmetry elements o^c

$$f(o^c \cdot o) = f(o) \tag{30}$$

As is also seen in Figure 15 the rotational symmetry elements operate "inside" each of the partial functions whereas the inversional ones lead from one to the other partial orientation space. This way it is possible to take all crystal symmetries uniquely into account.

It must be mentioned that in the enantiomorphic crystal classes the two functions f^r and f^i are independent of each other whereas in the non-enantiomorphic ones only one of them is independent.

It must also be mentioned that these considerations include the quasi-crystal symmetries additional to the 32 crystallographic symmetry classes.

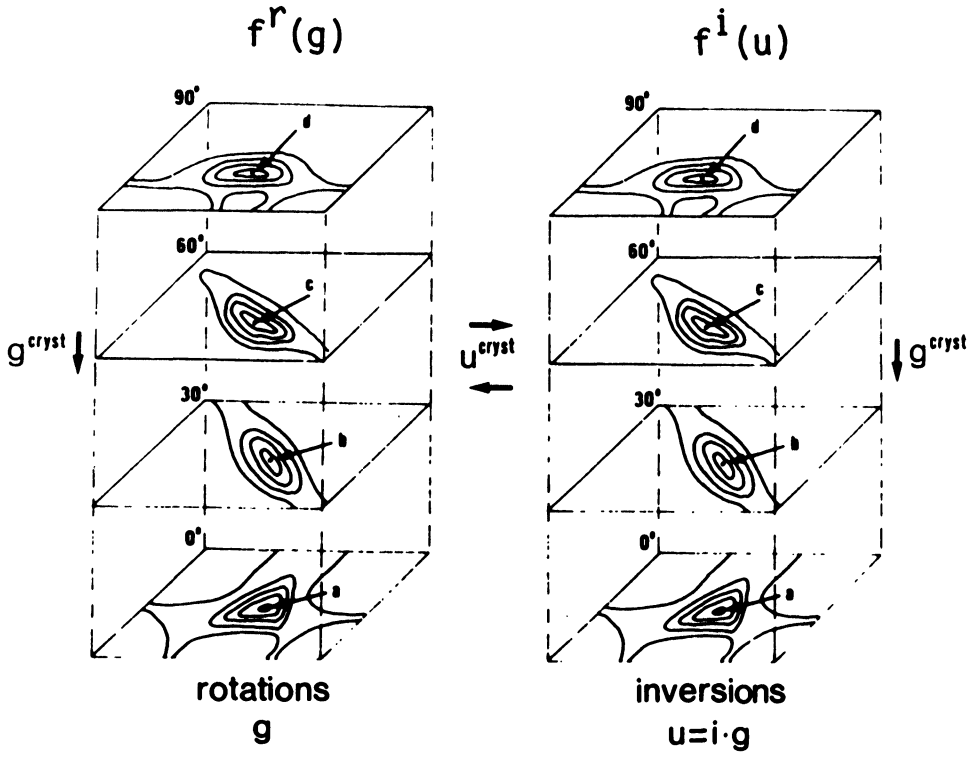

Figure 15 Two partial orientation distribution functions corresponding to rotational and inversional orientation parameters.

Sample symmetry

Besides the symmetry of the individual crystal we can consider symmetries in the arrangement of crystals. In the definition of the ODF the location of crystals is not considered, not even the very existence of individual crystals. Only the volume fractions of all crystals of the same orientation are considered. Hence, sample symmetry i.e. the symmetry of *arrangement* of crystals must be defined in this sense. It is a property of the *distribution function* rather than of individual crystals.

Symmetry in the orientation space SO(3)

In analogy to eq(30) we define sample symmetry by

$$f(o \cdot o^s) = f(o) \tag{31}$$

All orthogonal transformations

$$o^s \quad \begin{matrix} = g^s \\ = u^s \end{matrix} \tag{32}$$

fulfilling the identity relation eq(31) are considered as sample symmetries (strictly speaking eq(31) *defines* sample symmetry). Analogous to crystal symmetries, the symmetry rotations g^s operate "inside" the partial functions f^r and f^i whereas the inversional elements u^s lead from one to the other.

Contrary to crystal symmetry, sample symmetry - in principle - allows all point symmetry groups including all non-crystallographic ones. In fact, the non-crystallographic axial symmetries (i.e. rotation axes of infinite order) are particularly important.

Symmetries in the direction space S^2

Symmetry in a distribution function can also be defined in a more general way i.e. in the axis distribution function (Bunge, Esling, Muller 1980)

$$A(\vec{h}, \vec{y}) = \frac{1}{2} \int_{\vec{h}\|\vec{y}} f(o)\ \mathrm{d}\psi = \{A^r(\vec{h}, \vec{y}) + A^i(\vec{h}, \vec{y})\} \tag{33}$$

which can be split into two parts A^r and A^i according to eq(29). In this generalized sense, sample symmetry can be defined by

$$A(\vec{h}, o^s \cdot \vec{y}) = A(\vec{h}, \vec{y}) \tag{34}$$

Since this equation requires equality only for the sum of A^r and A^i and not for these partial functions individually it can be fulfilled in two essentially different ways with the sample symmetry elements o_1^s and o_2^s.

$$\begin{aligned} &A^r(\vec{h}, o_1^s \cdot \vec{y}) = A^r(\vec{h}, \vec{y})\ ;\ A^i(\vec{h}, o_1^s \cdot \vec{y}) = A^i(\vec{h}, \vec{y}) \\ &A^r(\vec{h}, o_2^s \cdot \vec{y}) = A^i(\vec{h}, \vec{y})\ ;\ A^i(\vec{h}, o_2^s \cdot \vec{y}) = A^i(\vec{h}, \vec{y}) \end{aligned} \tag{35}$$

Thereby $o_1^s = \{g_1^s, u_1^s\}$ and $o_2^s = \{g_2^s, u_2^s\}$ can be rotations or inversional elements. Comparing them with the ones of eq(31) it is found that

$$\begin{aligned} &\{g_1^s = g^s, u_2^s = u^s\} = o^s && \text{conventional sample symmetries} \\ &\{g_2^s, u_1^s\} = o^s{}_{non\text{-}conv.} && \text{non-conventional symmetries} \end{aligned} \tag{36}$$

The first ones are identical with the conventional symmetries of eq(31). The second ones g_2^s and u_1^s have no correspondence in the classical symmetries. Whereas the conventional symmetries eq(32) are one-to-one relations between orientations, the non-conventional ones can only be expressed in terms of *integrals over all orientations.*

In order to include both kinds of symmetries uniquely, black-white point-symmetry groups can be used (Bunge, Esling 1985). This is possible because of the fact that the product of two non-conventional symmetries is a conventional one

$$o^s{}_{non\text{-}conv.} \cdot o'^s{}_{non\text{-}conv.} = o^s \tag{37}$$

Also the non-conventional sample symmetries include all non-crystallographic black-white point groups.

Mathematical and physical aspects in symmetries

Crystal symmetry

Crystal symmetry is defined in the mathematical sense only for infinite ideal crystals containing no lattice defects (and ideally not even thermal vibrations). Physical crystals are real crystals. They have finite size, lattice defects, lattice strains and thermal vibrations. Hence, in the mathematical sense they have no symmetries at all (strictly speaking they are not even crystals in this sense).

With respect to texture analysis we have to take several symmetry-breaking effects in crystals into consideration. These are particularly:

- Shape of crystallites
- Atomic order in solid solutions
- Anisotropic distribution of dislocation substructures
- Strain
- Magnetization
- Electric polarization

These effects are not only anisotropic in the individual crystallite, thus breaking its ideal symmetry, they may also be different in crystals of different orientation. If we want to include these effects into our considerations, the definition of the ODF based on identical crystals with ideal symmetry, must be generalized. As an example we mention here "magnetic textures" (Bunge 1989) including the direction of spontaneous magnetization into the definition. In principle, the same holds for all above mentioned effects. At the time being, there are, however, only very few investigations studying systematically, for instance, the influence of crystallite shape or dislocation distribution on measured pole figures.

Hence, we usually assume that crystal symmetry is fulfilled with a high degree of accuracy although there may be strong deviations from this assumption. (see e.g. Perlovich in this volume.

Sample symmetry

We are much more aware of possible deviations from the ideally expected symmetry in the case of sample symmetry.

Sample symmetries are the consequence of symmetries of the texture-forming processes. Strictly speaking the resulting sample symmetry is the minimal symmetry common to all processes that have taken place during the whole "life" of the considered sample. As an example we may consider sample symmetries observed in sheet metals. They are dominated by the orthorhombic symmetry of the rolling process. However, the symmetry of the material before entering the rolls may have been lower so that the resulting symmetry from both processes is also lower. A prominent example for that is roll-casting which leads to only monoclinic symmetry after rolling. After rolling, recrystallization is often applied. This is (usually) an isotropic process which should conserve the symmetry existing prior to it. Hence, recrystallization textures in sheet metal are ideally also orthorhombic. Recrystallization may lead, however, to coarse (or even very coarse) grain size. The statistical sample symmetry can then only be fulfilled with the poor statistical relevance of this stage. If finally, another rolling process with orthorhombic symmetry follows, the bad statistics may pertain so that also after that rolling process strong statistical perturbations of the ideal orthorhombic symmetry may occur.

Symmetry degree ("Fuzzy" symmetries)

From the physical aspect, sample symmetry elements can only be considered with some degree of "fuzzyness".

With reference to the "mathematical" definition of sample symmetry eq(31) we introduce the "physical" definition of a "symmetry degree" η. For any particular symmetry element o^s we may define

$$\oint [f(o) - f(o \cdot o^s)]^n \cdot do = \eta_n(o^s) \tag{38}$$

(It may be mentioned that also other similar definitions of a symmetry degree may be used). For instance, Figure 16 shows schematically the symmetry degree η_1 for a mirror plane assumed at the angle α towards the rolling direction in a rolled sheet. It is seen that this quantity takes a minimum in the estimated symmetry position (i.e. the rolling direction) but it does not become zero as for mathematically exact symmetry.

One also sees that the symmetry degree for the mirror plane in transverse direction is different from that of the plane in rolling direction.

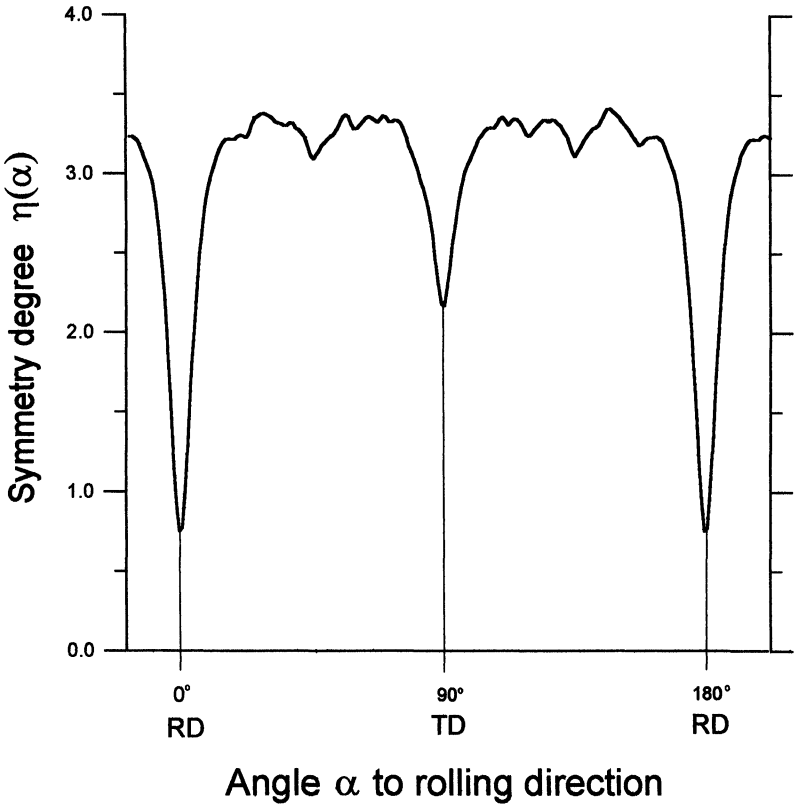

Figure 16 Symmetry degree η_1 showing the two mirror planes perpendicular to the sheet plane in a colled rolled copper sheet (schematical).

POLE FIGURE INVERSION

The calculation of the orientation distribution function $f(g)$ from pole distribution functions $P_{\vec{h}}(\vec{y})$ is called pole figure inversion.

The mathematical aspect

If we express the orientation g by the Euler angles $\{\varphi_1\phi\varphi_2\}$, the sample direction $\vec{y}$ by the pole figure angles $\{\alpha\beta\}$, and the crystal direction $\vec{h}$ by the Miller indices (hkl) of the plane perpendicular to it (distinguishing (hkl) and $(\bar{h}\bar{k}\bar{l})$ then the projection equation can be written in the form

$$P_{(hkl)}(\alpha\beta) = \frac{1}{2\pi} \int_{(hkl)\perp\{\alpha\beta\}} f(\varphi_1\phi\varphi_2)\, d\psi = A(\vec{h}, \vec{y}) \tag{39}$$

thereby ψ is the angle measured about the common direction $\vec{h}$ and $\vec{y}$. Eq(39) can be considered in two directions:

- from given f to any P (straight-forward)
- from given P to f (inverse problem)

The first problem has always a unique solution. The inverse problem has not always a solution. This may be easily seen in terms of the function $A(\vec{h}, \vec{y})$ which depends on two directions $\vec{h}$ and $\vec{y}$, each of which is described by two angular coordinates. Hence, $A(\vec{h}, \vec{y})$ is a four-dimensional manifold whereas $f(g)$ is only three-dimensional. Hence, if we choose a four-dimensional function $A(\vec{h}, \vec{y})$ deliberately eq(39) will, in general, not have a solution f. The function $A(\vec{h}, \vec{y})$ or the pole figures $P_{(hkl)}(\alpha\beta)$ will be "incompatible" in themselves. From the mathematical aspect this has been called an "ill-posed" problem (Volkov and Savyolova 1983).

If we deal with textures then we can assume that a sample *must* have an orientation distribution function f which gives rise to pole figures $P_{(hkl)}(\alpha\beta) = A(\vec{h}, \vec{y})$. Using these as "input values" the inverse problem has the solution f which is thus "reproduced" from the input pole figures $P_{(hkl)}(\alpha\beta) = A(\vec{h}, \vec{y})$. From the physical aspect this excludes, however, experimental errors in the pole figures which will (with only very rare exceptions) be incompatible with any solution f. In this case "reproduction" of the originally assumed function f will - strictly speaking - not be possible. Also, it will not be possible to find any other solution of eq(39). Hence, the term "reproduction" (Matthies 1979) is only meaningful for mathematically exact pole figures obtained from a given ODF f(g) by eq(39) in the forward direction.

The physical aspect

From the physical aspect the problem of eq(39) must be formulated differently. Usually we postulate

$$\sum_{(hkl)} \sum_{(\alpha\beta)} \left[P_{(hkl)}(\alpha\beta) - \frac{1}{2\pi} \int_{(hkl)\perp\{\alpha\beta\}} f^M(\varphi_1\phi\varphi_2)\, d\psi\right]^2 = Min \tag{40}$$

Thereby the sums run over all *available* (*hkl*) and all *available* values of ($\alpha\beta$). (In the limiting case the sums may be replaced by integrals over the four-dimensional $\vec{h}\vec{y}$-space). The mathematical nature of eq(40) is completely different from that of eq(39).

- Eq(40) has *always* a solution whatever may be the input function $P_{(hkl)}(\alpha\beta) = A(\vec{h}, \vec{y})$.
- The solution is (with some rare exceptions) always "practically" unique.

However:

- The solution depends on the used representation of the function $f^M(g)$ e.g. series expansion, discrete methods, or other.
- The solution depends on the model parameters e.g. series expansion degree L or choice of cells in the discrete methods.
- The solution depends on the available data points $(hkl)(\alpha\beta)$.
- The solution is not the "true" ODF

$$f^M \neq f^{true} \tag{41}$$

Two cases may be distinguished

$$\Delta f = |f^M - f^{true}| \quad \begin{cases} < \epsilon & \text{reliable solution} \\ > \epsilon \rightarrow \infty & \text{meaningsless solution} \end{cases} \tag{42}$$

In principle there is no strict way of telling which of both cases we deal with. In the case of using the series expansion method some empirical estimation of a *reliability range* may be given as is illustrated in Figure 17.

- If the used series expansion degree is too low (depending on the "sharpness" of the texture) then the model texture is smeared out with respect to the true texture.
- If the series expansion degree is too high (depending on the number of available input data) the solution may be "unstable".

(hkl) – ($\bar{h}\bar{k}\bar{l}$)-superposition (Ghost phenomena)

In conventional polycrystal diffraction experiments (*hkl*) and ($\bar{h}\bar{k}\bar{l}$) cannot be distinguished. Hence, eq(39) must be modified to (Matthies 1979)

$$\tilde{P}_{(hkl)}(\alpha\beta) = \frac{1}{4\pi}\left[\int_{(hkl)\perp\{\alpha\beta\}} f(g)\, d\psi + \int_{(\bar{h}\bar{k}\bar{l})\perp\{\alpha\beta\}} f(g)\, d\psi\right] = \tilde{A}(h, y) \tag{43}$$

Again we have to consider two directions in which to use eq(43)

- from given f to any $\tilde{P}$ (straight-forward)
- from given $\tilde{P}$ to f (inverse problem)

For the straight-forward problem there is no difference compared to eq(39).

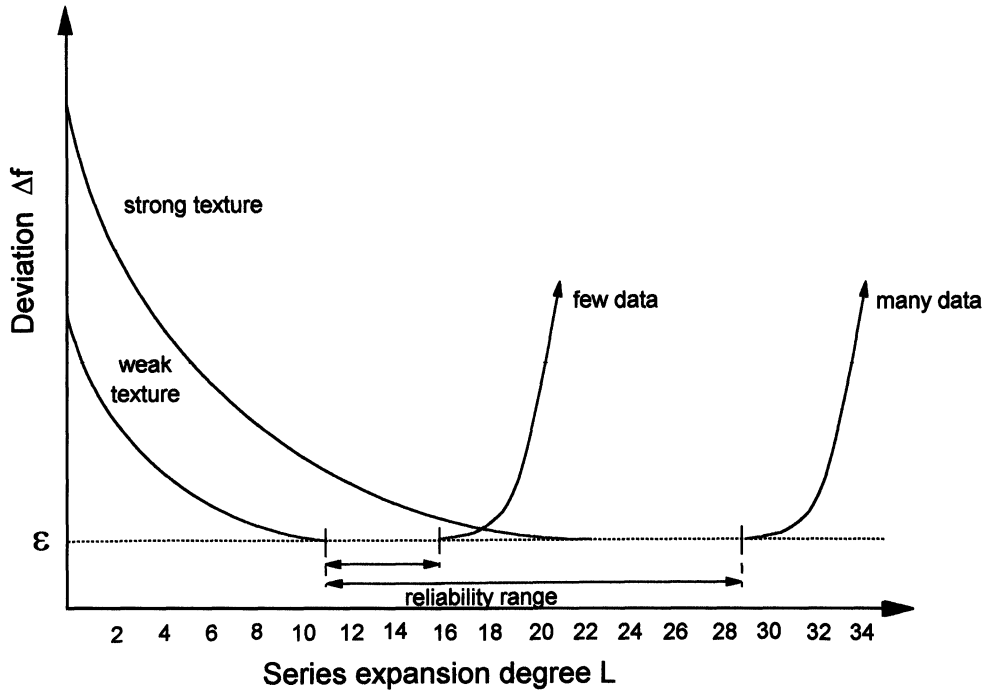

Figure 17 Definition of a reliability range of texture determination in terms of the series expansion method.

For the inverse problem the situation is similar to that of eq(39) in as far as it has no solution if $\tilde{P}_{(hkl)}(\alpha\beta) = \tilde{A}(h, y)$ is chosen deliberately. If the input function $\tilde{P}_{(hkl)}(\alpha\beta) = \tilde{A}(h, y)$ is "compatible" i.e. it corresponds to a particular $f(g)$ then the problem has a solution and many other solutions, too, (Matthies 1979) many of which contain, however, physically meaningless negative values Figure 18.

In this case eq(43) must be supplemented by the condition (Bunge, Esling 1979)

$$f(g) \geq 0 \tag{44}$$

Still the solution of eq(43) and eq(44) is not unique as is illustrated schematically in Figure 19. In the further treatment of this problem physical and mathematical aspects can be distinguished:

1) Physical aspects
   1.1 The experimental aspect.
   From this aspect it must be said that no further distinction can be made of solutions within the obtained solution band.

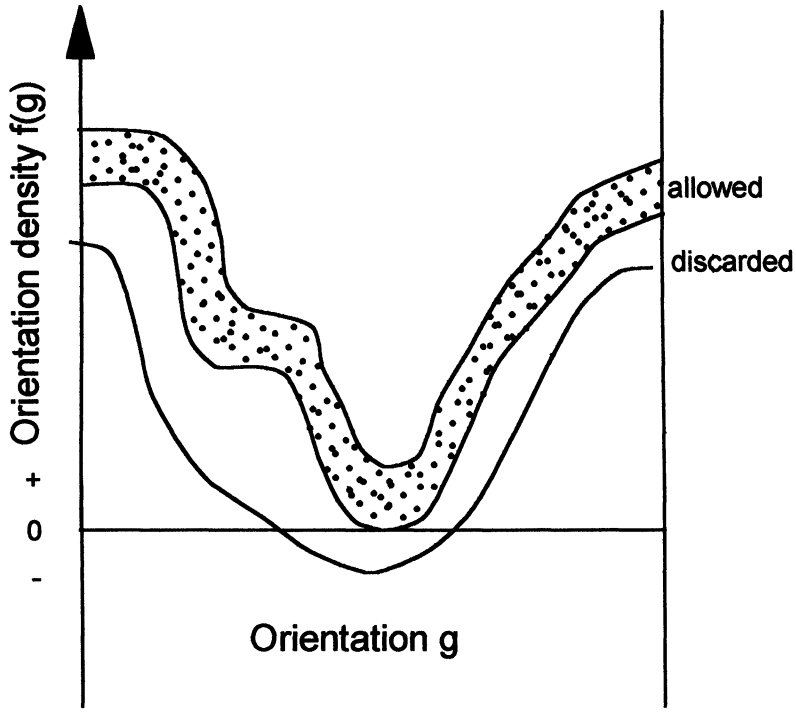

Figure 18 Range of solutions fulfilling eq(43) (schematical) and the restriction according to the positivty condition eq(44).

1.2 The texture formation aspect.
From the theory of texture formation processes we may know certain features of the function $f(g)$ e.g. that it should have a peak at g_o and, for instance, Gaussian spread about it.

1.3 The materials properties aspect.
If we know non-centrosymmetric physical properties e.g. piezo-electricity or optical activity of the textured polycrystalline material, then some odd-order series expansion coefficients can be determined from that. This does not yet fix the solution $f(g)$ completely but it may reduce the solution band.

2) Mathematical aspects
The mathematical aspect is strictly formulated by eq(43) and eq(44). This means the solution is not unique. Any particular function $f(g)$ within the solution band of Figure 19 is a possible solution to the problem.

2.1 Additional postulates

If a solution is not unique it allows to postulate further restricting conditions. It must, however, be emphasized that these are principally *postulates* which have, by themselves, no mathematical justification. Such postulates have been proposed several:

$$\oint [f(g)]^2 \, dg = Min \quad \text{Minimum Texture Index (Tavard 1977)} \tag{45}$$

$$\oint [f(g) \cdot \ln f(g)] \, dg = Min \quad \text{Maximum "Entropy"} \begin{pmatrix} \text{Schaeben 1988} \\ \text{Wang } et\ al \text{ 1988} \end{pmatrix} \tag{46}$$

$$f(g)_{min} = Max \quad \text{Maximum "Phone" (Matthies, Vinel 1982)} \tag{47}$$

$$f(g)_{max} = Max \quad \text{Maximum Peaks (Matthies, Vinel 1982)} \tag{48}$$

Strictly speaking, the addition of one of the equations eq(45) to eq(48) to the basic equations eq(43) and eq(44) defines four different mathematical problems which have different solutions as is illustrated schematically in Figure 19. Which one of these

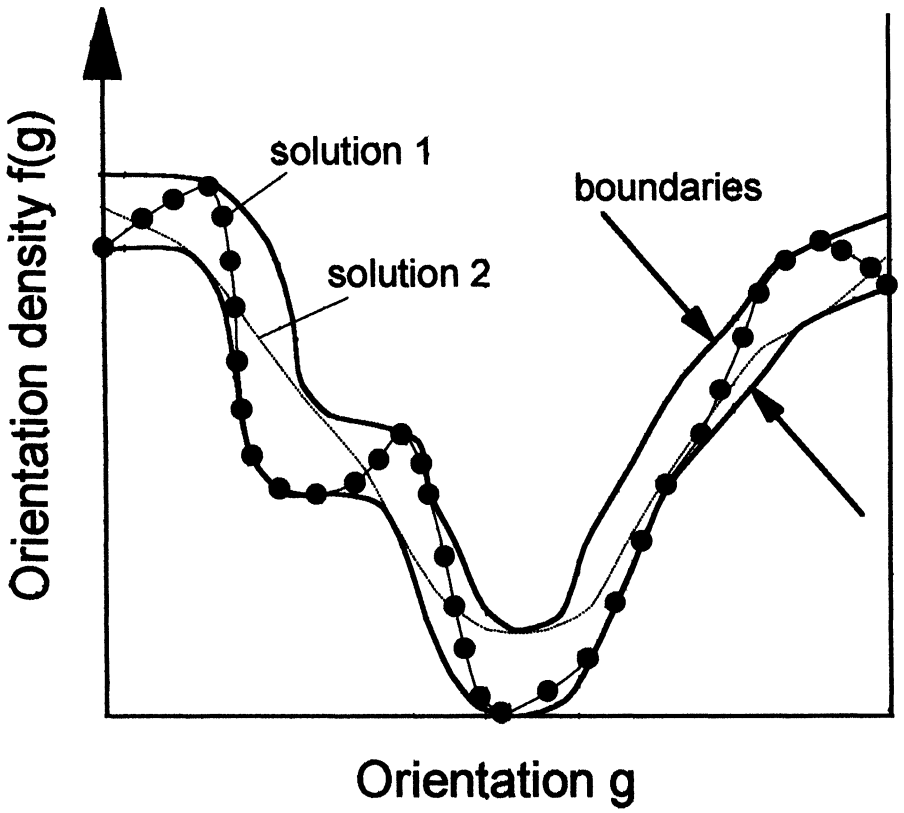

Figure 19 Choice of different solutions within the non-negative solution band.

mathematical problems really applies to the given situation must be decided from other than mathematical aspects. As a general rule it can be said that the solution band is the narrower the sharper the texture. Particularly, if the true texture has "zero-ranges" G_o

$$f(g) = 0 \qquad (g \in G_o) \tag{49}$$

these often lead to zero-ranges in the pole figures

$$\tilde{P}_{(hkl)}(\alpha\beta) = 0 \quad (hkl, \alpha\beta \in P_o) \tag{50}$$

In this case the solution can often be considered as being "practically unique" from the physical aspect (i.e. within the margin of experimental error).

Multipeak textures

Multipeak textures are characterized by individual orientations g_i in which the ODF has δ-character, the total intensity in the peak i being f_i. This ODF is projected by the projection equation eq(39) onto pole figure points $\{\vec{h}\vec{y}\}_j$ with the total intensity $A(\vec{h}\vec{y})_j$. The projection equation can then be written in the form (Bunge, Morris, Nauer-Gerhardt 1989)

$$A(\vec{h}\vec{y})_j = \sum_i a_{ij} \cdot f_i \tag{51}$$

where

$$a_{ij} = \begin{cases} 1 \text{ if } \{\vec{h}\vec{y}\}_j \text{ is consistent with } g_i \\ 0 \text{ if } \{\vec{h}\vec{y}\}_j \text{ is not consistent with } g_i \end{cases} \tag{52}$$

In order to solve eq(51) at first a set of g_i consistent with the observed set $\{\vec{h}\vec{y}\}_j$ must be found. This set may contain ghost orientations g_i^{ghost} which uncover themselves by the condition

$$f_i^{ghost} = 0 \tag{53}$$

It has not yet been studied thoroughly under which conditions eq(51) has a unique solution.

TEXTURE COMPONENTS

It is often considered desirable to rationalize a three-dimensional orientation distribution function by a relatively low number of parameters. This is possible with the concept of "texture components" which was the basis of the above-mentioned method of pole figure "interpretation" in terms of so-called "ideal orientations". These are orientations g_o at which peak intensity is observed and from which the intensity falls down according to some (not further specified) spread function. This concept was successfully used in the monograph by Wassermann and Grewen (1962). It works quite well if the texture consists of only a few (or even only one) relatively sharp such components which are separated from each other so that they do not merge into each other.

This Wassermann concept of components was defined in a qualitative way and as such it was very successful. It combines several aspects. These are among others:

- The crystallites of a component have nearby orientations and hence similar anisotropies of their properties.
- It may be assumed that the crystallites of a component have been brought into their orientations by the same physical process.
  This process is further understood as leading to an ideal orientation g_o which is, however, not reached completely (due to some disturbing effects) so that some spread about it occurs.
- The spread funciton can be described by a simple mathematical function.
  This facilitates the mathematical description of a component.
  It is also assumed that the form of the spread function follows from the physical process which formed this component.

In the Wassermann concept all these aspects were combined. This is justified as long as the concept is used in a qualitative way. Later on, it was tried to define "components" in a quantitative way. This requires to chose one of the above-mentioned aspects and to formulate a quantitative definition on its basis. Accordingly, several different definitions of "components" have been put forth and are presently being used. Sometimes this leads to some confusion if it is not clearly specified which definition is being used, and even more, if a "component" is at first specified according to *one* definition and is, later on, being used according to *an other one.*

The following different definitions of components may be distinguished:

COMPONENTS ACCORDING TO PHYSICAL ASPECTS

The property aspect - Vicinity components

According to this aspect crystals with nearby orientations and hence similar anisotropies of their properties are summarized into a component. Such a component may be called a "vicinity" component.

This still allows several different variants.

Maximum-distance components

Crystals of the orientations g deviating form the ideal orientation g_o by Δg are considered. The absolute value of Δg is limited to a chosen value ϵ.

$$g = \Delta g \cdot g_o \qquad \omega = |\Delta g| \leq \epsilon \tag{54}$$

For ϵ, values between 5° and 10° are often considered. This is illustrated in Figure 20. The advantage of this definition is that it includes only crystals which are really near enough to the ideal orientation g_o.

The disadvantage is that the choice of ϵ is deliberate and that the spread function about g_o may be cut off. Also, it may leave orientations which do not belong to any so defined component.

Voronoi cells

According to this definition a set of ideal orientations g_i is chosen. Any orientation g is considered as belonging to its *nearest* ideal orientation g_i

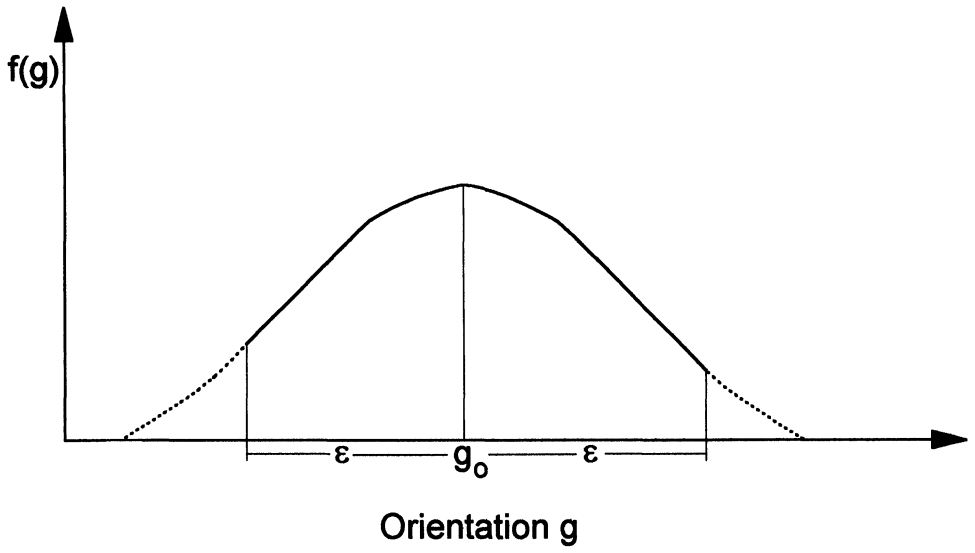

Figure 20 Definition of maximum-distance components.

$$g = \Delta g_i \cdot g_i \qquad \omega_i = \cdot |\Delta g_i| \leq Min \tag{55}$$

This is the definition of Voronoi cells (Voronoi 1908). A one-dimensional example is shown in Figure 21.

The advantage of this definition is that each orientation belongs uniquely to a component.

Disadvantages are that the definition of an individual component depends on all other components. Also the maximum distance in a component may be different in different directions.

Minimum intensity boundaries

Another possible definition is to place the boundary between the components g_i, and g_j into the local intensity minimum between the two maxima in g_i and g_j, This is also illustrated in Figure 21.

The advantage of this definition is that it seems to be "most natural". The disadvantage is that it may lead to complicated boundaries in the three-dimensional orientation space and that the positions of the boundaries may depend on the *intensities* of the components.

All variants of "vicinity" components have in common that they are mainly being used in order to replace all orientations g belonging to a component by the central orientation g_o and then to calculate physical properties with this orientation g_o.

This may be an acceptable approximation as long as the orientation distribution function $f(g)$ is not known. It is, however, an unacceptable approximation if at first $f(g)$ was known from which subsequently the components were deduced. In this latter case the concept of "anisotropy components" is to be preferred since it leads to exact values of the properties and not only to approximations.

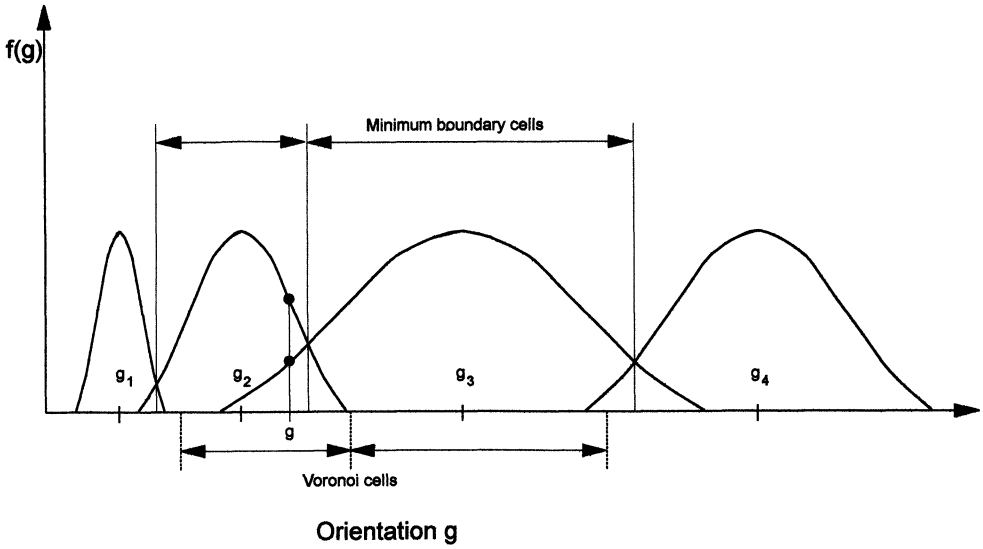

Figure 21 Voronoi and minimum-intensity cells. The orientation g belongs to two components at the same time.

The texture formation aspect - Process components

According to this aspect crystals brought into orientation by the same physical process are considered as belonging to a component. In principle this requires that we have a model of the process or the processes which have formed a particular component. This is often not the case.

The advantage of this definition is that it is closely related to model calculations of texture forming processes. The disadvantage is that it often leads to overlapping spread functions from different ideal orientations as is also illustrated in Figure 21. In this case, one and the same orientation g may belong to different components.

As an example, Figure 22 shows the distribution functions in the vicinity of the (111) and (200)-orientation respectively in a recrystallized Al-wire. It is seen that the (200)-distribution can be well described by a Gauss-function whereas the (111)-distribution is distinctly different.

The symmetry aspect - Anisotropy components

If the texture is represented in terms of a series expansion with the coefficients $C_\lambda^{\mu\nu}$ then it turns out that the macroscopic anisotropy depends only on a few coefficients $C_\lambda^{\mu\nu}$. This is illustrated in Figure 23 for fourth-order properties in cubic materials with orthorhombic sheet symmetry. In this case the macroscopic anisotropy may be decomposed into four components i.e.

- isotropic component
- cylindric
- 2-fold
- 4-fold

} symmetry

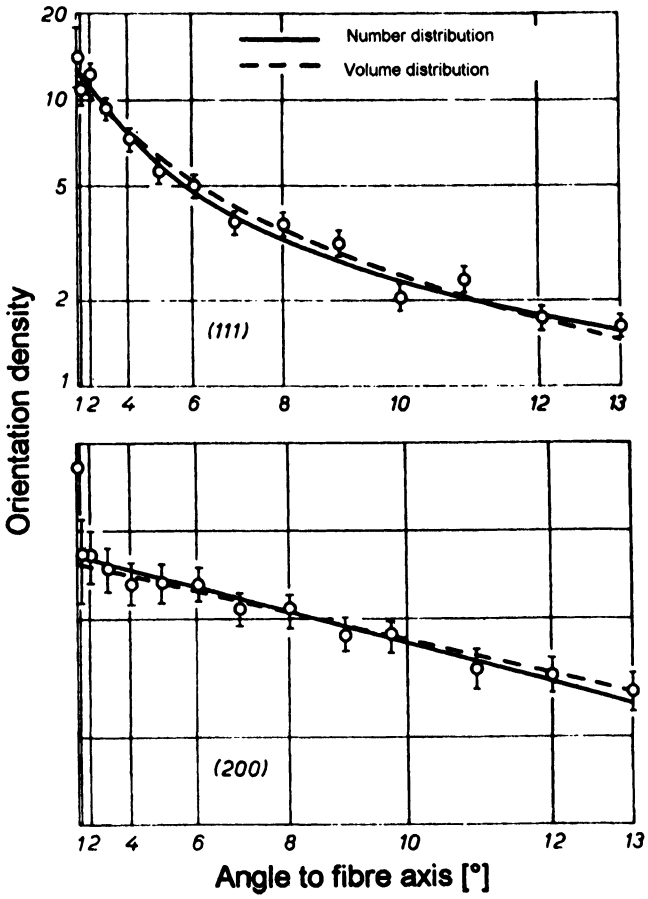

Figure 22 Spread functions of the orientation distribution in the vicinity of the ideal orientations (111) and (200) in a recrystallized aluminium wire. The (200)-distribution is "Gaussian" the (111)-distribution is not.

The texture coefficients are expressed by

$$C_\lambda^{\mu\nu} = \oint f(g) \cdot \overset{\cdot\cdot}{T}{}_\lambda^{\mu\nu}(g)\, dg \tag{56}$$

Hence, in a somewhat different meaning, we may call an orientation distribution function $\overset{\cdot\cdot}{T}{}_\lambda^{\mu\nu}(g)$ a "symmetry component".

The advantage of this definition is that it allows to calculate the macroscopic properties exactly, i.e. without the approximation mentioned in the case of "vicinity" components.

The disadvantage of this definition is that it does not say anything about individual crystals in individual orientations and that a so-defined symmetry component contains negative values (except the isotropic component). Hence, these components cannot be considered individually. They are meaningful only in combination.

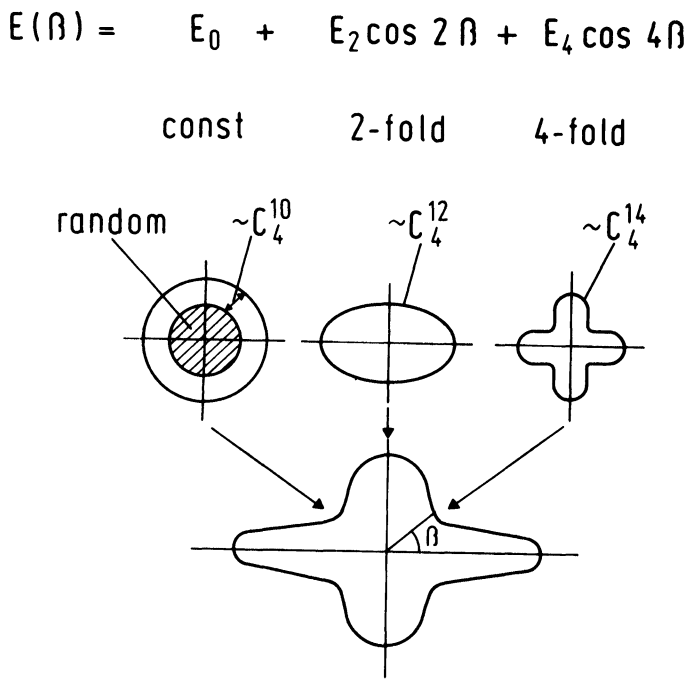

Figure 23 Anisotropy components of a fourth-order property in an orthorhombic sample.

COMPONENTS ACCORDING TO MATHEMATICAL ASPECTS

"Functional" components

The definition of a component assumes that the highest intensity is reached in the "ideal" orientation g_o. In a mathematical aspect, components can then be distinguished according to the mathematical type of the spread function about g_o. This problem has been discussed in great detail in the literature (see e.g. Savyolova (1984), Schaeben (1992), Bucharova, Savyolova (1993)). Particularly, this discussion rises the question which type of function is "normal" in the sense that a "normal" spread is added to an "ideal" physical process. As is seen, however, in Figure 22 that such "normal" spread cannot be expected from a physical point of view.

Central functions

Spread functions depending only on the orientation distance $\omega = |\Delta g|$ have been called "central functions".

The Gauss function has the form

$$f^G(g,\ g_o,\ \omega_o) = N(\omega_o) \cdot e^{-\left(\frac{\omega}{\omega_o}\right)^2} \quad ;\ \omega = |g \cdot g_0^{-1}| \tag{57}$$

This function can be easily expressed in terms of the texture coefficients $C_\lambda^{\mu\nu}$

$$C_\lambda^{\mu\nu} = a_\lambda(\omega_o) \cdot T_\lambda^{\mu\nu}(g_o) \tag{58}$$

$$a_\lambda = \frac{\exp[-\frac{1}{4}\lambda^2 \cdot \omega_o^2] - \exp[-\frac{1}{4}(\lambda+1)^2 \cdot \omega_o^2]}{1-\exp\ [-\frac{1}{4}\omega_o^2]}$$

The Standard-function (Matthies 1982, Matthies, Vinel, Helming (1987) has the form

$$f^s(g,\ g_o,\ s) = N(s) \cdot e^{-s \cdot \cos\omega} \quad ;\ \omega = |g \cdot g_0^{-1}| \tag{59}$$

It can also be expressed in terms of the coefficients $C_\lambda^{\mu\nu}$

$$C_\lambda^{\mu\nu} = a_\lambda(s) \cdot T_\lambda^{\mu\nu}(g_o) \tag{60}$$

with $a_\lambda(s)$ expressed in terms of modified Bessel functions.

The two functions eq(57) and eq(59) were compared by Matthies, Muller, Vinel 1988.

Elliptical functions

These are "non-central" spread functions in the meaning that they do not only depend on $\omega = |\Delta g|$ but also on the spread direction. On the basis of the standard function eq(59) the elliptical spread function

$$f^E(g,\ g_o,\ \boldsymbol{s}) = N(\boldsymbol{s}) \cdot e^{-s \cdot \cos\omega} \tag{61}$$

can be defined where now $\boldsymbol{s}$ is a matrix with six components (Eschner 1993). It describes the principal spread directions and the spread values in these directions. An example where this model proved to be very well applicable is shown in Figure 24. It is the cold rolling texture of copper which could be very well represented by the components $\{112\} < 111 > + \{110\} < 112 > + \{110\} < 001 >$ with appropriate spread matrices $\boldsymbol{s}$ and volume fractions (see Eschner 1994)). Other three-axial spread functions were introduced by Dnieprenko and Divinski (1993).

Cylindrical components (fibre components)

Besides ideal orientations g_o (with spread about them) also "cylindrical" texture components (fibre axes) have been considered (Wassermann and Grewen (1962)). These latter authors also considered "limited fibre axes". These are essentially elliptical components with one axis much longer than the other two. Hence, the elliptical components are the most general concept including fibre components if one of the axes of the matrix $\boldsymbol{s}$ becomes infinitely long.

Volume fractions of components

If a texture consists of several components then it can be expressed in the form

$$f(g) = \sum_i f_i(g) = \Sigma V_i \cdot f_i^M(g), \quad \Sigma V_i = 1 \tag{62}$$

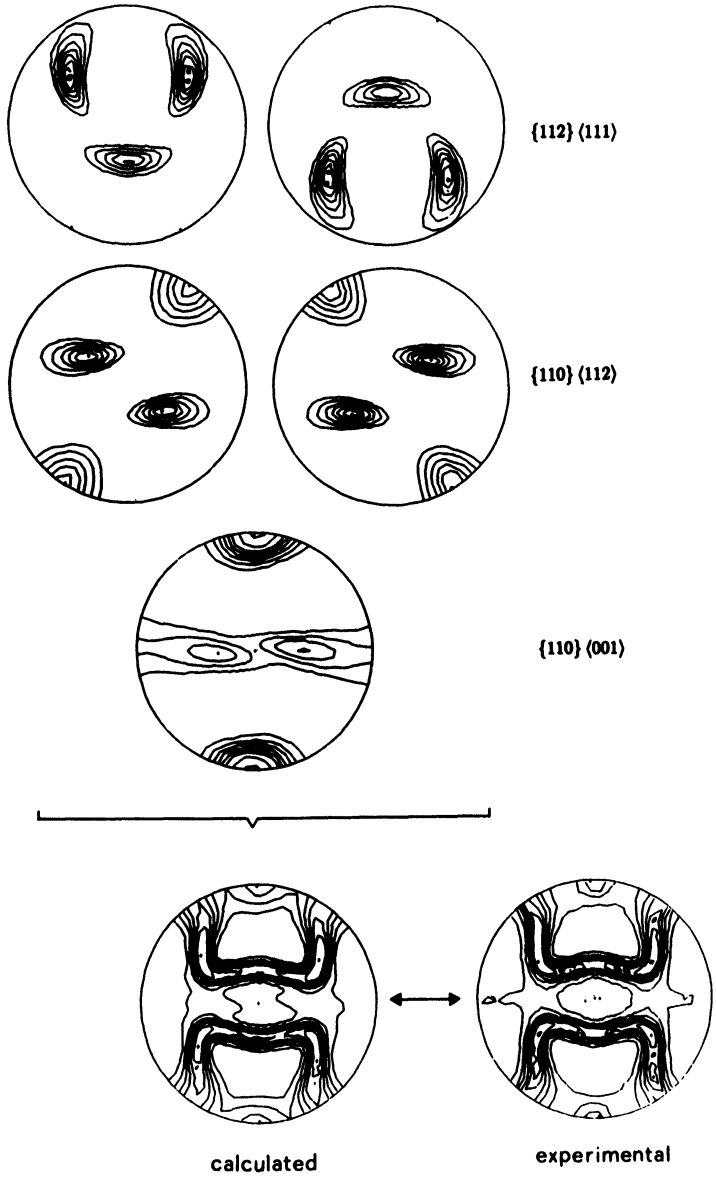

Figure 24 Composition of the rolling texture of copper by three (resp. five) elliptical components.

where $f_i(g)$ are the parts of the texture belonging to each component i. The $f_i^M(g)$ are the normalized distribution functions and V_i are the volume fractions. The volume fractions are given by the integral over $f_i(g)$

$$\int_{(comp.)} f_i(g)\ dg = V_i \qquad \int_{(comp.)} f_i^M(g)\ dg = 1 \tag{63}$$

where the integral is to be taken over the component. This expression takes on two different variants depending on whether we use one of the "vicinity" components or one of the "functional" components:

$$V_i = \int_{vicinity} f(g)\ dg \tag{64}$$

$$V_i = \oint f_i(g)\ dg \tag{65}$$

In the latter case a component i extends formally through the whole orientation space although its numerical values may converge very rapidly. In this latter case, the contribution of the long tails of the spread function may be considerable. Small differences of these tails even *below the experimental accuracy* may thus contribute strongly to the volume fraction. This may lead to strong errors particularly when the so defined volume fraction is used in the meaning of a "vicinity" component in order to calculate properties (corresponding to the ideal orientations g_i). It may also lead to errors when the so defined volume fractions are considered in texture formation models.

Remainder components

It must be kept in mind that only some of the definitions of components lead to volume fractions which sum up to unity. Strictly speaking this applies only to the Voronoi components.

The maximum-distance components usually leave gaps between them which may, however, contain crystals, too, which then do not belong to any component. Strictly speaking this "remainder" component does not have random orientation distribution. For simplicity reasons it is, however, often approximated by a random distribution. Also "functional" components do not necessarily sum up to unity depending on how they are being fitted to the experimental texture.

Random component - Phone

Because of these reasons, mostly a "random" component is included in eq(62) in order that the volume fractions sum up to unity. The definition of a random component, also called "phone" maybe quite different.

- In the maximum distance model it equals the "remainder" component.
- In the "functional" models it is added to the distribution functions. Since these functions often overlap the "phone" component is difficult to distinguish in this case.
- Another definition of the "phone" component is by the minimum of the texture function

$$f_{phone} = Min\ [f(g)] \tag{66}$$

The component-fit method

Another mathematical aspect of "components" is used in the "component-fit" method as a particular pole figure inversion method (Helming, Eschner 1990). Here it is assumed that the texture can be uniquely decomposed into components according to eq(62). It is further assumed that each component function $f_i^M(g)$, introduced into the projection equation eq(39) leads to distinguishable components in all (or at least some) pole figures $P^M_{(hkl)}(\vec{y})_i$. The pole figure components are then fitted to the experimental pole figures

by a least squares fit according to eq(40), however extending the $\alpha\beta$ sum only over the range of each component separately. This procedure can be done interactively thus allowing to include the "intuition" of the operator as a heuristic principle for an easy way to find the solution.

It must be mentioned that this method works very well if the texture indeed consists of only a low number of distinct components. It has also been successfully applied with many components. In this case it is, however, not necessarily mathematically unique.

SUMMARY AND CONCLUSIONS

In Figure 1 the main physical aspects in the field of textures and their attributed mathematical requirements were illustrated. The central part is the definition of texture (as well as generalized textural quantities) by statistical parameters of a stochastic polycrystalline aggregate. The definition of these quatities is limited by the angular resolving power and statistical relevance which are related to each other. Mathematical concepts reaching beyond this limit are thus not meaningful from the physical point of view.

The central quantity in textures is crystal orientation which is represented in an orientation space with non-euclidean metric. This requires mathematical methods of dealing with such spaces particular if higher-dimensional spaces must be considered e.g. for the generalized textural quantities. Texture measurement e.g. by polycrystal diffraction, gives rise to the projection problem which must be solved mathematically. The conditions for solutions and their properties may be judged quite differently from the mathematical and physical points of view.

Finally, texture and higher-order textural quantities play an essential role in physical models and their mathematical formulation trying to understand the process by which polycrystalline aggregates are formed as well as the macroscopic properties of such aggregates. In these models physical and mathematical aspects are insolvably interwoven. In the present paper a few of the physical and mathematical aspects in texture analysis and their mutual correlations were given some consideration.

References

Bucharova, T. I. and Savyolova, T. I. (1993). Application of Normal Distributions on $SO(3)$ and S^n for Orientation Distribution Function Approximation. *Textures and Microstructures,* **21**, 161–176.

Bunge H. J. (1965). Zur Darstellung allgemeiner Texturen. *Z. Metallkunde*, **56**, 872–874.

Bunge, H. J. (1969). Mathematische Methoden der Texturanalyse. Akademie-Verlag Berlin.

Bunge, H. J. (1982). Texture Analysis in Materials Sciences. *Mathematical Methods*. Butterworths Publ. London.

Bunge, H. J. (1989). Texture and Magnetic Properties. *Textures and Microstructures,* **11**, 75–91.

Bunge, H. J. (1994). Statistical Crystallography of the Polycrystal. *Textures of Materials*. ICOTOM-10 Materials Science Forum, **157–162**, 13–30 TransTech Publ. Switzerland.

Bunge, H. J. and Esling, C. (1979). Determination of the Odd Part of the Texture Function. *Journal de Physique, Lettres*, **40**, 627–628.

Bunge, H. J., Esling, C. and Muller, J. (1980). The Role of the Inversion Centre in Texture Analysis. *J. Appl. Cryst.*, **13**, 544–554.

Bunge, .H. J. and Esling, C. (1985). Symmetries in Texture Analysis. *Acta Cryst.*, **A 41**, 59–67.

Bunge, H. J., Morris, P. and Nauer-Gerhadt, C. N. (1989). ODF-Analysis of Multipeak Textures. *Textures and Microstructures*, **11**, 1–22.

Bunge, H. J. and Weiland, H. (1988). Orientation Correlation in Grain and Phase Boundaries. *Textures and Microstructures*, **7**, 231–264.

Dnieprenko, V. N. and Divinski, S. V. (1993). A New Approach to Describing Three-Dimensional Orientation Distribution Functions in Textured Materials. *Textures and Microstructures*, **22**, 73–85.
Eschner, Th. (1993). Texture Analysis by Means of Model Functions. *Textures and Microstructures,* **21**, 139–146.
Eschner, TH. (1994). Quantitative Texturanalyse durch Komponentenzerlegung von Beugungspolfiguren. Ph. D. Thesis Freiberg.
Esling, C., Bunge, H. J. and Muller, J. (1980). Description of Texture by Distribution Functions on the Space of Orthogonal Transformations. *Journal de Physique, Lettres*, **41**, 543–545.
Hansen, J. Pospiech, J. and Lücke, K. (1978). Tables for Texture Analysis of Cubic Crystals. Springer Verlag Berlin.
Helming, K. and Eschner, T. (1990). A New Approach to Texture Analysis of Multiphase Materials Using a Texture Component Model. *Cryst. Res. Technol.*, **25**, K 203–208.
Matthies, S. (1979). On the Reproducibility of the Orientation Distribution Function of Texture Samples from Pole Figures, (ghost phenomena). *Phys. Stat. Sol.*, (b) **92**, K 135–138.
Matthies, S. (1982). Aktuelle Probleme der quantitativen Texturanalyse. Akademie der Wissenschaften der DDR ZFK-Rossendorf 480.
Matthies, S., Muller, J. and Vinel, G. W. (1988). On the Normal Distribution in the Orientation Space. *Textures and Microstructures*, **10**, 77–96.
Matthies, S. and Vinel, G. W. (1982). An Example Demonstrating a New Reproduction Method of the ODF of Texturized Samples from Reduced Pole Figures. *Phys. Stat. Sol*, (b) **(112)** K 115–120.
Matthies, S. Vinel, G. W. and Helming, K. (1987). Standard Distributions in Texture Analysis. Akademie-Verlag Berlin.
Perlovich, Yu. Some Physical Errors of X-Ray Texture Measurements. (This volume).
Roe, R. J. (1965). Description of Crystallite Orientation in Polycrystaline Materials. III General Solution of Pole Figure Inversion. *J. Appl. Phys.*, **36**, 2024–2031.
Savyolova, T. I. (1984). Distribution Function of Grains with Respect to Polycrystal Orientations and its Gaussian Approximation. Zavodskaya Laboratoriya, **50**, 48–52 (Russian).
Schaeben, H. (1988). Entropy Optimization in Quantitative Texture Analysis. *J. Appl. Phys.*, **64**, 2236.
Schaeben, H. (1992). "Normal" Orientation Distribution. *Textures and Microstructures,* **19**, 197–202.
Tavard, C. and Royer, F. (1977). Indices de Texture partiels des Solides Polycristallins et Interpretatin de l'Approximation de Williams C.R. *Acad. Sci. Paris,* **284**, 247.
Volkov, N. G. and Savyolova, T. I. (1983). The Incorrect Formulation of a Problem in Crystal Physics *J. Numerical Math. and Math. Phys.*, **23**, 922.
Voronoi, G. (1908). Recherches sur les paralleloedres primitives. Journ. Reine und Angew. *Math.*, **134**, 198–287.
Wang, F., Xu, J. and Liang, Z. (1988). Inverse Pole Figure Determination According to the Maximum Entropy Method. Proceedings ICOTOM-8 111–114 Eds. J. S. Kallend and G. Gottstein The Metallurgical Society, Warrendale.
Wassermann, G. (1939). Texturen metallischer Werkstoffe. Springer Verlag Berlin.
Wassermann, G. and Grewen, J. (1962). Texturen metallischer Werkstoffe. Springer Verlag Berlin.
Williams, R.,O. (1968). Representation of the Textures of Rolled Copper, Brass and Aluminium by Biaxial Pole Figures. *Trans. Met. Soc. AIME*, **242**, 104–115.